

EFFECT OF SURFACE CHARGING ON DC FLASHOVER CHARACTERISTICS OF POLYMERIC INSULATORS

By

IMTIAZ RIFANUL HOQUE
SHAHID ALAM

Diploma Work No. 73/2011

Department of Materials and Manufacturing Technology
CHALMERS UNIVERSITY OF TECHNOLOGY
Gothenburg, Sweden

Master Thesis in ELECTRIC POWER ENGINEERING

Performed at: Chalmers University of Technology
SE-41296 Gothenburg, Sweden

Supervisor: Tech. Lic. Sarath Kumara

Examiner: Associate Professor Yuriy Serdyuk
Department of Materials and Manufacturing Technology
Division of High Voltage Engineering
Chalmers University of Technology
SE-41296 Gothenburg, Sweden

Effect of Surface Charging on DC Flashover Characteristics of Polymeric Insulators
IMTIAZ RIFANUL HOQUE
SHAHID ALAM

© **IMTIAZ RIFANUL HOQUE**, 2011
© **SHAHID ALAM**, 2011

Diploma work no 73/2011
Department of Materials and Manufacturing Technology
Division of High Voltage Engineering
Chalmers University of Technology
SE-41296 Gothenburg, Sweden
Telephone + 46 (0)31-772 1000

Chalmers Reproservice
Gothenburg, Sweden 2011

Effect of Surface Charging on DC Flashover Characteristics of Polymeric Insulators
IMTIAZ RIFANUL HOQUE
SHAHID ALAM
Department of Materials and Manufacturing Technology
Chalmers University of Technology

ABSTRACT

Nowadays polymeric insulators are widely replacing the traditionally used glass and porcelain based insulators. They have become dominant in HVDC transmission systems operating at high voltage levels such as 800 kV. The withstand performance of polymeric insulators in relation to impulse flashover characteristics was extensively studied during the last couple of decades and quite broadly documented in the literature. The knowledge on dc flashover characteristics of polymeric insulators, in combination with the surface charge accumulation, is needed to be developed and it is a topic of ongoing research.

The research within the master thesis project focused on studying dc flashover characteristics of cylindrical polymeric insulators affected by pre-deposited surface charges by using theoretical analysis and experimental investigations. The study was conducted on cylindrical polymeric insulator samples made of a glass fiber reinforced epoxy core covered with a layer of silicone rubber and placed between metallic electrodes with rounded smooth edges. To reflect practical situations where surface charges may appear due to partial discharges in air, a dc corona belt was developed to deposit surface charges on the insulators. The influences of various parameters such as charging voltage magnitude, time duration, polarity and position of the corona belt on the surface charging were investigated. Charging of insulators due to pre-stressing by high applied voltages and by preceding flashovers was also investigated. The surface potential measurements were carried out using Kelvin type potential probe to register the amount of charges on the surface. The results obtained, both for surface potential measurements and the effect of surface charges on dc flashover characteristics of cylindrical polymeric insulators are discussed and presented in the report.

Keywords: surface charges, dc corona charging, material properties, surface potential measurements, surface potential decay, dc flashover voltage.

ACKNOWLEDGMENTS

The project work related to the effect of surface charging on dc flashover characteristics of polymeric insulators was carried out at the Division of High Voltage Engineering at Chalmers University of Technology.

First and foremost our utmost gratitude goes to our examiner, Associate Prof. Yuriy Serdyuk for his valuable guidance, inspiration and most of all for his patience. He had motivated us to do more by bringing new ideas and finally shaping our report. Our thanks must also go to Prof. Stanislaw Gubanski, Head of Division of High Voltage Engineering, for his valuable advice and support.

We would also like to extend our gratitude to our supervisor Sarath Kumara for his guidance, help and providing valuable information during the measurement period. He also helped us a lot for analyzing the simulation results using Comsol software. We divided the work load equally and we both had equal contribution in the whole thesis project.

At last, but not least, we would like to thank our family, our colleagues here in the department and our friends for their invaluable support and inspiration to continue this study abroad.

Imtiaz Rifanul Hoque & Shahid Alam
Gothenburg, Sweden 2011

TABLE OF CONTENTS

CHAPTER 1: INTRODUCTION.....	1
1.1. Background	1
1.2. Objectives of the thesis	1
1.3. Outline of the thesis	1
CHAPTER 2: LITERATURE REVIEW	3
2.1. Surface charging of polymeric insulators	3
2.1.1 Physical background.....	3
2.1.2 Corona charging of polymers	4
2.2. Surface charge decay	6
2.3. Methods of surface charge measurements	7
2.4. Effect of surface charges on flashover characteristics of polymeric insulators	9
CHAPTER 3: SURFACE CHARGING OF POLYMERIC INSULATOR.....	11
3.1. Experimental setup	11
3.2. Preliminary studies	15
3.3. Experimental results	18
3.4. Surface potentials due to pre-stressing	18
3.5. Surface potentials due to preceding flashovers	20
3.6. Surface potentials due to external corona	21
3.7. Surface potentials due to pre-stressing and external corona	22
3.8. Surface potentials due to preceding flashover and external corona	23
3.9. Surface potential decay measurements and interpretation	24
CHAPTER 4: SIMULATION OF SURFACE CHARGING OF POLYMERIC INSULATORS	27
4.1. Model description	27
4.2. Results.....	29
4.2.1 Charging by external corona	29
4.2.2 Pre-stressing only.....	30
4.2.3 Surface charges due to pre stressing and external corona	31

CHAPTER 5: EFFECT OF SURFACE CHARGES ON DC FLASHOVER CHARACTERISTICS OF CYLINDRICAL POLYMERIC INSULATORS	33
5.1. Experiment setup and procedure	33
5.2. Experimental results.....	33
5.2.1 Preliminary studies.....	33
5.2.2 Flashover voltage with charges from previous flashover event	34
5.2.3 Flashover voltage with pre-stressed sample.....	35
5.2.4 Measurement of flashover voltage without corona charging	36
5.3. Flashover voltages in presence of charges deposited by external corona	37
5.3.1 Flashover voltages with charges from preceding flashover and corona.....	37
5.3.2 Flashover voltage with charges from pre-stressing and external corona.....	38
5.3.3 Flashover voltage with charges from corona only	39
 CHAPTER 6: CONCLUSIONS AND FUTURE WORK.....	 41
6.1. Conclusions	41
6.2. Future work.....	42
 REFERENCES	 43
 APPENDIXES	 45
Appendix A.....	45
A1: Position study.....	45
A2: Charges from pre-stressing and corona	48
A3: Charges from previous flashover and corona	49
A4: Neutralization study.....	50
A5: Decay in first 3 minutes.....	51
A6: Surface potential at different sides of the insulator sample.....	52
A7: Live scanning at -10 KV.....	53
 Appendix B.....	 54
FOV Values	54
Reference FOV Values	55
 Appendix C.....	 55
Matlab Codes	55

CHAPTER 1: INTRODUCTION

1.1. Background

Technical advantages of polymeric insulators over the traditionally used glass and porcelain based ones have stimulated their applications in diverse high voltage technologies, in particular, as outdoor insulation especially for HVDC power transmissions. Despite of the fact that technical and technological properties of polymeric insulators have been studied extensively, there is still a lack of knowledge on some practical aspects, in particular, flashover mechanisms in presence of surface charges. Surface charging is an inherent phenomenon in HVDC systems and may strongly affect performance of polymeric materials. Charge accumulation and its distribution along the insulator surface are key issues to be understood as the charge deposition alters the electric field along the surface and thus affecting the flashover characteristics. Therefore, this phenomenon should be considered while designing and co-coordinating insulation systems, where polymeric insulators should function properly under operating conditions and also be able to withstand overvoltages to insure the reliability of power delivery.

Most of the studies related to the effect of surface charges on flashover characteristics reported in the literature have been conducted with impulse test voltages and only few of them have been performed under DC conditions. This thesis presents results of the investigations on surface charging of model polymeric insulators and on their DC withstand performance under different charging conditions

1.2. Objectives of the thesis

The MSc thesis project was conducted aiming to analyze performance of model polymeric insulators charged by pre-stressing and external corona discharges and to understand the influence of charging parameters (voltage magnitude, polarity, duration, etc.) on surface charge behavior. The goal of the project was to establish regularities in DC flashover characteristics of cylindrical polymeric insulators due to pre-deposited surface charges based on theoretical study and experimental observations.

1.3. Outline of the thesis

The report is divided into six main chapters:

Chapter 1 presents the background and objectives for carrying out the master thesis project.

Chapter 2 presents a literature survey on surface charging mechanisms, highlights nature of the surface charge accumulation on polymeric materials. Effects of various parameters on surface charging, measurement techniques and influences of surface charges on dc flashover characteristics of polymeric insulators are discussed.

Chapter 3 presents the experimental method used for corona charging of cylindrical polymeric insulators and analyses effects of charging voltage magnitude, polarity, duration and position of the corona belt on surface potential profiles measured on polymeric insulators.

Chapter 4 presents the simulation model, technique and results related to the conversion of the measured surface potentials into charge densities.

Chapter 5 focuses on the effect of surface charges on the dc flashover characteristics of cylindrical polymeric insulators. The effect of surface charges under different scenarios such as charges from previous flashover, pre-stressing and corona on the flashover characteristics are discussed in this chapter.

Chapter 6 presents the conclusions and suggestions for the future work.

CHAPTER 2: LITERATURE REVIEW

This chapter presents the literature review on surface charging of polymeric insulators and its effect on the flashover characteristics.

2.1. Surface charging of polymeric insulators

Surface charging of polymeric materials have been studied extensively. Despite of this, there still unclear questions arising from practical use of polymeric insulators related to surface charge deposition, its distribution along the surface, charge behavior with respect to time, different factors influencing the surface charge accumulation etc. It is believed today that phenomena associated with surface charge accumulation involve several physical mechanisms (polarization and conduction, external discharges, etc.) and each of them may become dominant under certain conditions [1, 2, 3].

2.1.1 Physical background

Polymeric materials are composed of long chains of molecules. Depending on the arrangement of the chains or parts of them, a polymer can be classified as a crystalline or as an amorphous state. In general, a polymer contains both crystalline and amorphous regions. The crystalline portion is called lamellae. The lamellae grow as spokes of a bicycle form a central nucleus. The whole assembly of spokes forms a structure which is called spherulite. Crystalline structures are never perfect. The surface of polymeric materials behaves as discontinuity of long chains. This discontinuity results in the formation of surface traps (regions of lower potential energy) where external charges may reside during long time. From the previous work of several authors [4, 5] related to charge trapping it has been made possible to show that on a polymeric material there are both deep and shallow surface traps. The authors proposed that the ions generated e.g. in a corona discharge, once come to the surface of polymeric materials, can either stay as stable entities on the surface or according to the energy states of the ions and surface, electrons transfer might occur to neutralize the ions, thus charging the surface state of the polymer.

Accumulated surface charge results an electric field in the dielectric material as well as in the surrounding gaseous medium. The field strength can be evaluated by using Gauss law, which states that-

“The electric flux density through any surface is proportional to the enclosed electric charge”

Gauss law may be expressed in its integral form as

$$\oint_S \mathbf{E} \cdot d\mathbf{A} = \frac{Q}{\epsilon_0} \quad 2.1$$

The left hand side of the equation represents the electric flux through the closed surface S. Gauss law in the differential form can be written as

$$\nabla \cdot \mathbf{E} = \frac{\rho}{\epsilon_0} \quad 2.2$$

Where ρ is the charge density and the left hand side represent the divergence of the electric field.

2.1.2 Corona charging of polymers

The research related to surface charging conducted during last couple of decades have been mostly focused on corona charging of polymeric materials. Different techniques for corona generation have been used in order to control surface charge uniformity and other parameters like sample voltage etc. In practice, deposition of charges on polymeric surfaces can be also achieved by e.g. exposing a polymeric insulator to high voltages, partial discharges in the surrounding gases, internal charge development due to inhomogeneity in the insulating material properties [6] etc. However, the discussion below is limited to corona charging.

Corona is a self-sustainable, non-disruptive electrical gas discharge. The threshold for the corona discharge depends on the availability of free electron which can trigger an electron avalanche. If the avalanche length surpasses a critical length X_c , the space charge developed in the head due to ionization have the capability to change into a channel of plasma (streamer) which can extend in both directions (anode and cathode). From measurements [7], it has been found that transformation from avalanche to streamer occurs when the charge within the avalanche head reaches a critical value $n = \exp(\alpha X_c) = 10^8$ where α is the ionization co-efficient and X_c is the critical avalanche length.

For non-uniform fields, such as between fine wire or point and a plate or cylinder, the streamer causes corona discharge. The streamer inception criteria for a non-uniform field can be mathematically represented as [7] $\int_{x_c} \alpha(x) dx \geq 18 - 20$.

Corona discharge for a point to plane geometry is shown Fig 2.1-1. The sharp point (high electric field) causes ionization of the gas molecules in the vicinity and the drift region extend towards the plane which is at lower potential. Several authors have elaborated the theory of charge drift towards the low field electrode under both positive and negative coronas [8, 4, 9].

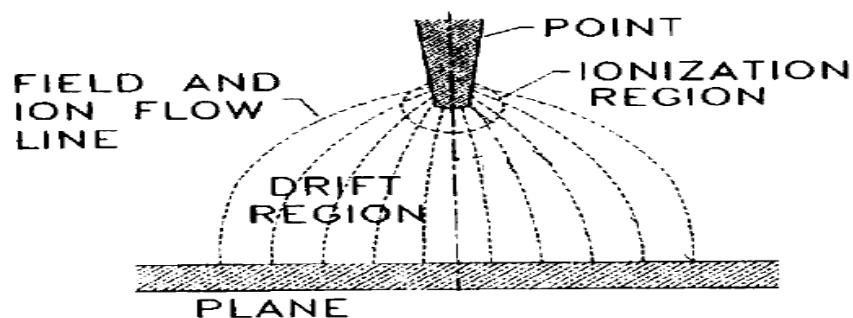


Figure 2.1-1: Corona discharge in the point to plane geometry [8]

If a polymeric material is placed in a corona region, generated charge carriers are trapped on its surface. Thus In [9], charge accumulation on polymeric surface was studied in a point-plane electrode arrangement under positive glow corona and burst pulse corona both experimentally and using numerical simulations. Charge deposition was found to be a continuous process in glow corona, whereas in case of burst corona a series of positive charge clouds contributed to the surface charge deposition.

The nature of the generated ions for both positive and negative corona depends on the nature of the gas [8]. Spectrometer techniques have been used by several authors [10, 11] to identify types of generated ions for both positive and negative coronas. It was found [8] that in air, the dominant species in positive corona with respect to the relative humidity were $(H_2O)_nH^+$, where the integer n increases with relative humidity. At low humidity, other species such as $(H_2O)_nNO^+$ and $(H_2O)_n(NO_2)^+$ become dominant. For negative corona, the dominating ions were CO_3^- type and at 50% of relative humidity about 10% of the ions are in the hydrated form $(H_2O)_nCO_3^-$. Thus, effects of the environmental factors such as humidity, temperature and pressure on the nature of generated ions in the vicinity of the corona treated materials are important to investigate, so that to find the correct ion species deposited on the polymeric surfaces.

Traditionally used point-plane arrangement for charging polymeric samples offers less control over the surface charge uniformity. In order to achieve higher values of surface charges and more control over their uniformity, an improvement was the advent of a corona triode, which consists of a corona tip, a metallic grid and a sample holder. A simple arrangement of the corona triode is shown in Fig 2.1-2.

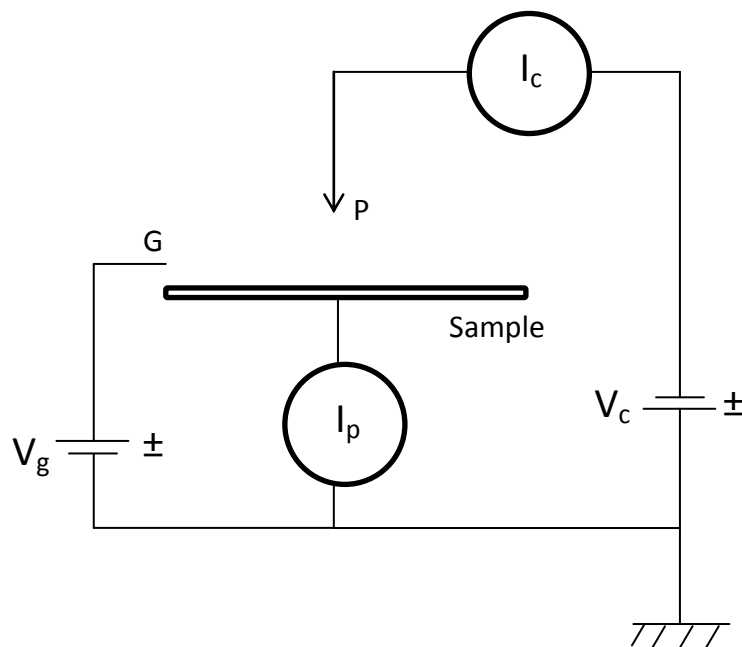


Figure 2.1-2: Schematic diagram of a corona triode

In this arrangement, a metallic point P is connected to the high voltage source V_c to produce ions which drift towards the material sample. A grid, biased by voltage supply V_g , is also inserted in the point to sample gap in order to control the surface charging. The corona triode arrangement is used to charge the sample and the current I_p become zero when the

surface potential on the sample becomes equal to the grid voltage. It is particularly useful when studying flat samples, however requires significant modifications to be adapted for other configurations. In the present work, cylindrical insulators are analyzed and direct corona charging is utilized.

2.2. Surface charge decay

Surface charges deposited on polymeric materials may be neutralized in some way that leads to a decay of their density. Surface charge decay measurements can be used as a technique to diagnose the dielectric properties. Over the last couple of decades, results of charge decay measurements on different materials have been published and various mechanisms have been proposed to describe related physical processes, e.g., charge transport within the material, charge spreading over the surface, etc. [4, 5].

Bulk neutralization and gas neutralization were proposed to be the dominant mechanisms for surface charge decay [12]. Some of the authors also suggest that surface charge/potential decay may not be caused by charge injection into the bulk rather neutralization may happen due to compensation of the arrival of charges of opposite polarity to the sample surface. The arrival of charges of opposite polarity to the charged surface has been studied in [13]. Several other mechanisms, like charge migration along the surface where humidity play an important role, and conduction through the bulk have also been proposed by different authors. Though it is not clear which mechanism is more dominant, it is a point of worth to explore the relative importance of each mechanism.

Information related to electrical properties like charge storage, charge transport along the surface and other decay mechanisms can be obtained by measuring the surface charge (potential) decay by means of an electrostatic voltmeter or other techniques like thermally simulated current (TSC) or thermally simulated depolarization, heat pulse techniques etc [8].

Several mechanisms for surface charge decay have been proposed by different authors and yet require more knowledge to explore the relative importance of each of them.

Bulk neutralization

Bulk neutralization happens due to the intrinsic conduction, polarization processes, charge injection and trapping in the bulk of the material. The recent theories about the surface charge decay are based on the hypothesis of charge injection into the bulk of the material (bulk conduction) accompanied by slow process of volume polarization [14]. Intrinsic conduction depends on the charge carrier generation, recombination as well as their mobility within material bulk. Intrinsic conduction under low fields and moderate temperatures is often considered as zero [15]. The slow polarization processes is predominant at lower fields (long time decay).

Surface conduction

Surface conduction refers to the charge leakage along the surface, it is highly field dependent process (the surface current is usually zero at low fields) [15]. The leakage current take place due to tangential component of electric field and is quantified by the

parameter, surface conductivity [12]. This mechanism mostly dominates during the initial stage of surface charge decay [15].

Gas neutralization

Gas neutralization refers to the arrival of charges of opposite polarity to the sample surface. Charge injection at the interfaces also takes place at high levels of initial field. Free ions of different polarities exist in the air due to various background ionization processes. Electric field caused by the surface charges can lead to the possibility of arrival of free ions which results in the reduction of surface potential. Concentration of free ions, strength of electric field in the vicinity of charged sample and energy depths of surface state are critical factors which determines the efficiency of surface charge decay due to gas neutralization [12].

2.3. Methods of surface charge measurements

The presence of electrostatic charges on the surface of polymeric materials can be detected by measuring different parameters on the surface such as electric field, electrostatic potential or charge density. There is a broad variety of instruments which can measure electrostatic charges and potentials through contact or contactless methods. If time behavior of surface charges is of interest, potential probes such as electrostatic fieldmeters and voltmeters are used [16].

Polarity and distribution of charges can be determined by using electrostatic powder that is a mixture of two different types of particles, .e.g., talc and jewelers' rough. The powder, when put on a surface that is positively charged, attracts talc particles while rough particles are attracted to surfaces with opposite polarity. Surface charge measurement by this technique give only qualitative information of the charge polarity and surface charge distribution but lacks the information about surface charge decay and other parameters [16].

The development of capacitive probes has put forward a very fast, inexpensive and cheap method of surface potential measurement. Electrostatic fieldmeters and voltmeters belong to the category of devices that are used for surface potential/charge measurement [17]. A simple diagram of a capacitive probe is shown in the Fig 2.3-1.

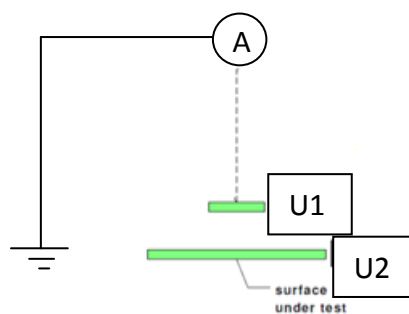


Figure 2.3-1: Schematic diagram of a capacitive probe

The principal of operation was first introduced by Kelvin. The working principle of capacitive probe is to detect the charge quantity electrostatically induced on the detective plate of probe.

The capacitance of the above arrangement in air is given by the mathematical equation

$$C = A\varepsilon/d \quad 2.3$$

Where $\varepsilon = \varepsilon_0\varepsilon_r$, A is the area of the vibrating Kelvin sensor and d is the distance between the sensor and the surface under test. In Fig 2.3-1 U_1 and U_2 corresponds to the potentials on the probe and the charged sample respectively. The potential difference between the probe and charged sample is represented by $U = |U_1 - U_2|$. In order to find the voltage between the probe and charged sample, let the potential difference to be constant. Since U_2 and the area of the probe are constant, so by changing the distance d , the capacitance can be changed. As potential on the probe is the ratio of charges, electrostatically induced on the detecting plate of probe, to the capacitance. So by changing the capacitance, the charges on the probe should change accordingly to keep the potential U_1 constant. By measuring the current and the distance d , it is possible to find out the potential between the probe and the charged sample [16]. The sensitivity of such devices should be high enough to detect a small magnitude of currents.

Another method called “field-nulling technique” has been developed, which is mostly used for flat charged samples. In this method a variable voltage source is applied to the probe. When the probe voltage becomes equal to the charged sample voltage the current approaches to zero. Zero current detection means that the probe voltage is the same as the charged sample voltage. As gradient of the potential define the electric field, so zero potential difference means no electric field. A simple diagram for “field-nulling technique” is shown in the Fig 2.3-2.

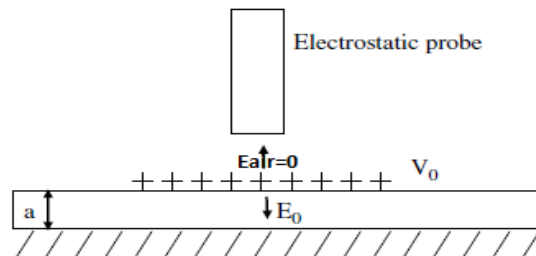


Figure 2.3-2: Electrostatic potential measurement by means of an electrostatic probe [28]

Although measurements of charges accumulated on solid insulator surfaces by electrostatic voltmeters are a fast and inexpensive method, it has certain limitations for certain applications. In [18], surface charge measurement on a spacer in +500 kV DC-GIS is performed by a capacitive probe inside a gas tank. The measurements performed through capacitive probe included some errors (which depends on the distance between the dielectric and grounded plate, thickness of the dielectric, area of the surface charging, distance between the probe and dielectric, bulk charging etc). An analytical method based on extending a three dimensional surface charge method, was developed to correct the measurement error and transform the probe potential to the surface charge distribution. The charge distribution obtained through analytical method was compared with dust figures to investigate the inaccuracies in the capacitive probe measurement.

In [17], surface charge measurement through electrostatic voltmeter and fieldmeter was made for a circular plate of area of 310 cm^2 , stressed to 1 kV, and the comparative error with respect to the distance from the sample was plotted for both the instruments to show the inaccuracy in the measurement. The fieldmeters have comparatively poor spatial resolution, require relatively larger test surfaces and large probe to surface distance to obtain accurate results. The electrostatic voltmeters have higher spatial resolution and may be used for measurements on small test surfaces and at small probe to surface distances.

2.4. Effect of surface charges on flashover characteristics of polymeric insulators

Effect of magnitudes, polarity and positions of charges pre-deposited by corona discharges on the flashover performance of polymeric insulators under impulse voltages has been studied for the last couple of decades and various conclusions have been put forward for different insulating materials [19, 20, 21].

Charge accumulation on the polymeric insulator surface can vary due to the change in the electrical parameters like magnitude, polarity and time duration of the applied voltage and due to the environmental factors like humidity, pressure and temperature [19, 8]. Since the change of any of these parameters can alter the charge magnitude and its distribution along the surface, so as a consequence change the electric field and thus the flashover voltage. In [20], EPDM and silicon rubber samples of different chemical composition have been exposed to standard lightning impulse flashover voltages (FOV) in combination with the pre-deposited surface charges of both positive and negative polarity. The experimental results showed that charges of the same polarity as the applied impulse caused a reduction in the flashover voltage compare to the case when both charges and applied impulse were of the different polarity.

In [21], the flashover voltages were calculated through a numerical model and results were compared with the experimental observations obtained in [20]. The comparison showed that the numerical model have a maximum of 11% deviation from the experimental results.

In [19], an attempt was made to analyze the effect of both the magnitude and location of deposited charges on the flashover performance of polymeric insulators by means of numerical simulations. It was shown in the report that the increasing magnitude of negative deposited charges leads to a linear increase of the impulse FOV for positive polarity, while a non-linear behavior was found when both the charges and the applied impulse voltages were positive. The position of the charged spot on the surface of both the positive and negative charges with respect to positive applied impulse voltages were also shown in the report. The explanation for the effects of both the magnitude and location of deposited charges were put forward with the help of calculating the electric field under each scenario. For negative charges, the impulse flashover voltage increased as the charge spot was moved away from the live electrode (anode). In case of positive charges, a decrease in the impulse flashover voltage was observed for charge spot closer to the grounded electrode while closer to the live electrode and in the middle of the insulating surface the charge spot caused an increase in the flashover voltage.

CHAPTER 3: SURFACE CHARGING OF POLYMERIC INSULATOR

This chapter focuses on the experimental procedure of surface charge deposition through corona discharges in air. The influence of various parameters like amplitude, duration, polarity and positions of the corona source on the surface potential distribution are investigated.

3.1. Experimental setup

The experiments were performed on cylindrical polymeric insulators shown in Fig. 3.1-1. The sample consisted of a glass fiber reinforced epoxy core (108 mm length, 30 mm diameter) covered with 4 mm thick layer of silicone rubber and placed between metallic electrodes with rounded smooth edges. The properties of the materials are given in the table. The insulating body was placed between two metallic electrodes with rounded edges and was fixed by plastic screws.



Material	Relative permittivity	Conductivity (Ωm) ⁻¹
Epoxy core	4	10^{-14}
Silicone Rubber layer	3.5	10^{-14}
Air	1	10^{-15}

Figure 3.1-1: Photograph of the sample and the materials parameters [26]

The experimental setup consisted of three different systems for charging the insulator, for measuring surface potential distributions and for dc flashover testing. The latter was also used for charging of the insulator by pre-stressing. The charging time was kept about two minutes throughout the experiments for both the external corona and pre-stressing.

The experimental setup for charging of composite polymeric insulator by corona discharge is shown in Fig 3.1-2. The corona charging belt was made of two semi-circular plastic supports which carried 27 needles mounted symmetrically. The length of each needle was 38 mm with tip radius of about 125 μm . The diameter of the corona charging belt was about 90 mm and the distance between the needles and the sample surface was about 23 mm. The distance between the needles was kept about 1 cm in order to achieve similar charging conditions within a circular area on insulator surface. The needles were connected to a dc source which provided up to ± 20 kV dc voltage. The metallic electrodes were kept grounded during charging. After charging for two minutes, the dc voltage source was turned off and

the corona belt was grounded and was removed within 10sec. Surface potential measurement was started at 60 sec after charging.

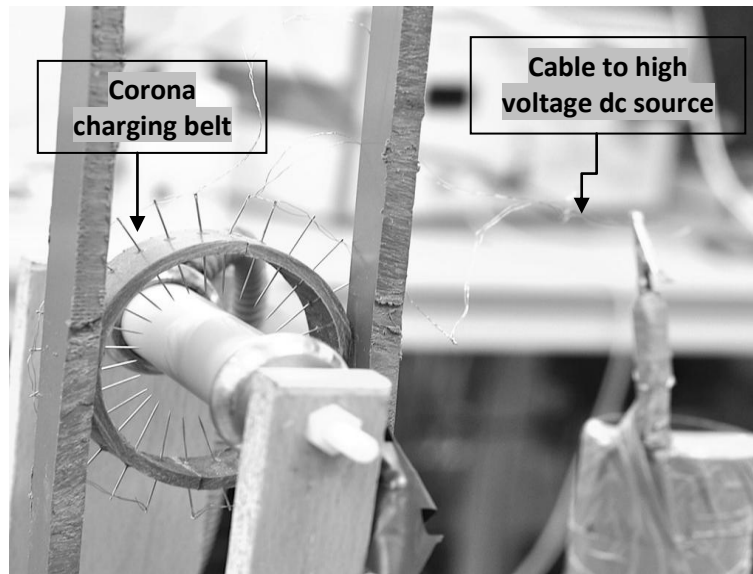


Figure 3.1-2: Arrangement for charging of polymeric insulator using corona belt

The setup used for recording surface potential distributions is shown in the Fig 3.1-3 and Fig 3.1-4. The measurements were performed using a vibrating capacitive probe connected to an electrostatic voltmeter (Trek model 341B or 347). The distance between the probe and the sample was kept at 2 mm to achieve accurate results. The voltmeter provided a low voltage replica (attenuated by 1000 times) of the probe potential. A voltage divider was used to further step down the signal to a ratio of 4:1 to make it possible for data acquisition system to handle it. A linear positioning system together with its controller was used to move the probe in both x- and y-directions. A shielded connector block received signals for the position and surface potential during the scanning from the robot controller and electrostatic voltmeter, respectively, and communicated with computer through a data acquisition (DAQ) card. A measurement program shown in Fig 3.1-5 and written using Labview software was used to acquire, display and record the data, received through DAQ card, continuously. Sampling rate was set to 5 samples/ sec using parameters setting in the DAQ assistance express.

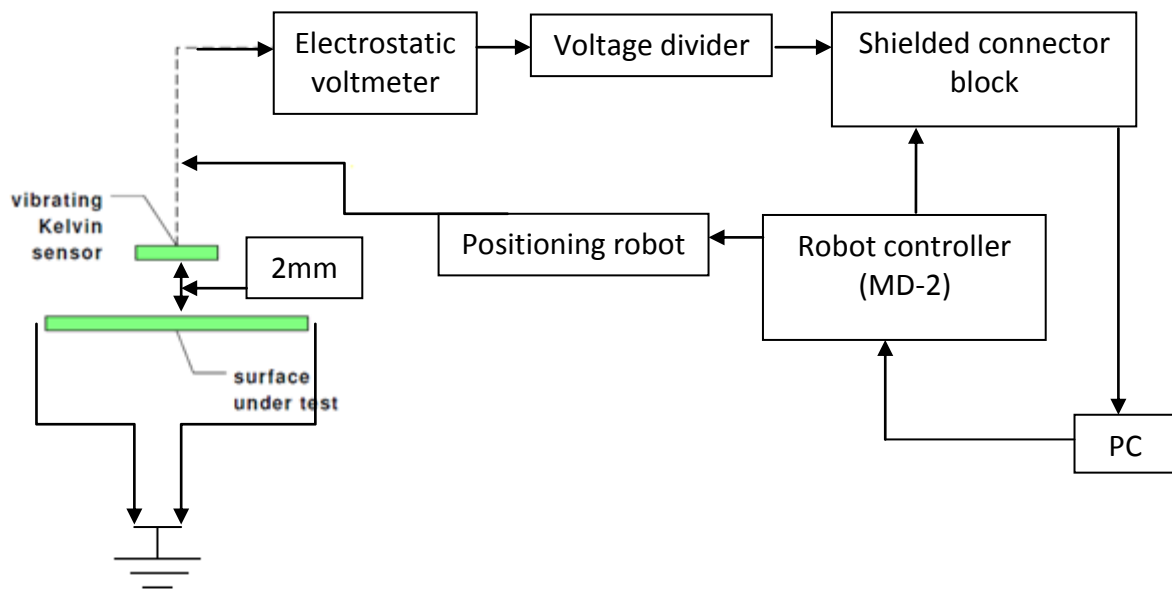


Figure 3.1-3: Scanning setup for surface potential measurement on a corona charged sample

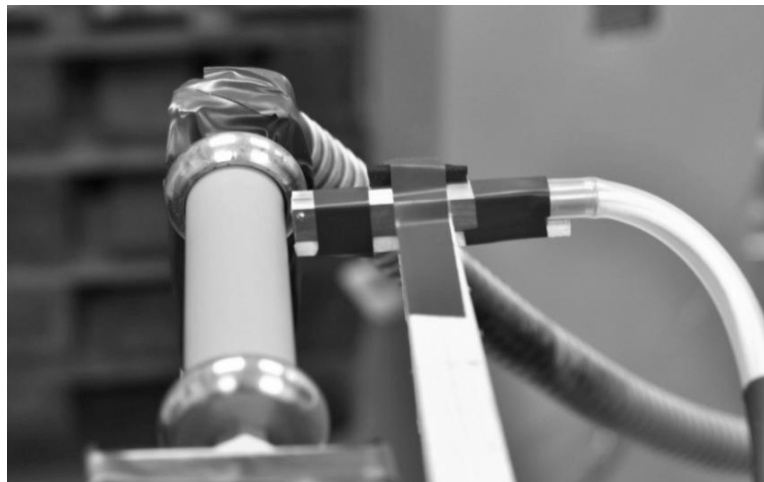


Figure 3.1-4: Surface potential measurement by capacitive probe

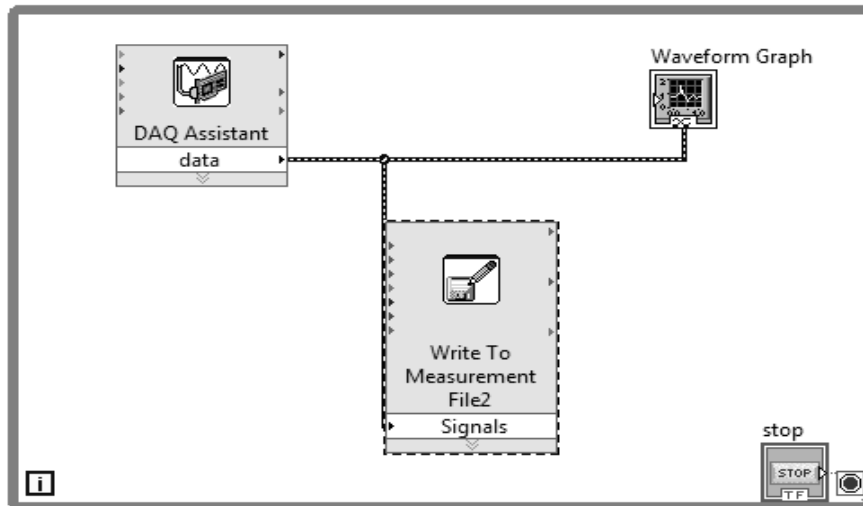


Figure 3.1-5: National instruments software LabView, parameter settings

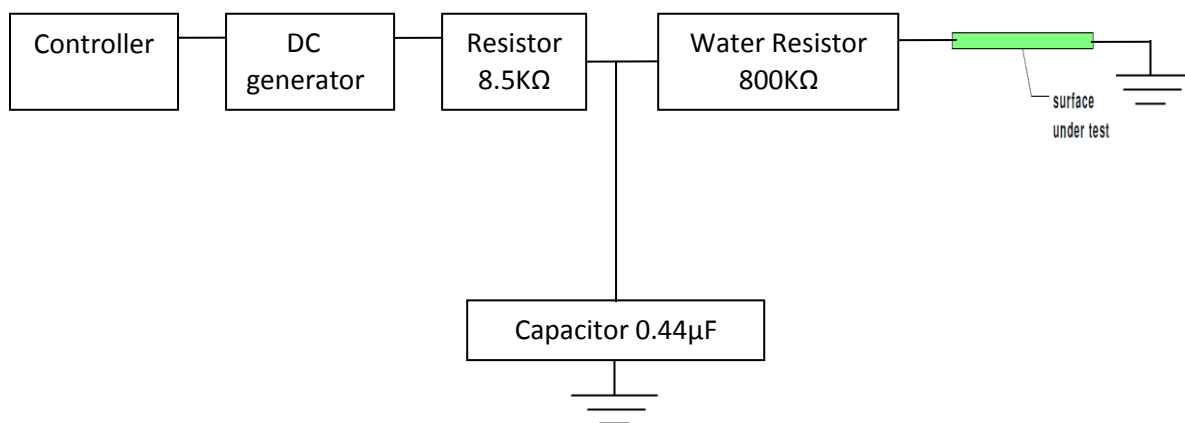


Figure 3.1-6: Schematic view of charging arrangement of polymeric insulator through pre-stressing

The software supplied with the positioning robot arm controller was used to program the probe motion in such a way to move it from one end of the sample to the other end with predefined stops at certain position. A graph was plotted between the surface potential values, taken from the recorded data, and effective length of the sample to get the corresponding surface potential for each position along the surface.

The experimental setup for flashover testing shown in Fig 3.1-6 consisted of a dc generator of type CBQE 100/1800, where 100/1800 represents the voltage and current ratings of the dc generator in kV and mA respectively. The generator provided only negative dc voltages. The inbuilt controller was used to regulate the magnitude and rate of rise of the output voltage. A capacitor of 0.44 μF with the withstand rating of 100 kV was used to smooth out the voltage output of the generator. A water resistor and 8.5 kΩ resistor were used to limit the current output of the generator during charging and discharging. During the tests, one of the electrodes was kept grounded and the negative dc voltage was applied to another one.

3.2. Preliminary studies

The preliminary studies were performed initially to investigate the effect of charging time, belt position and magnitude of the charging voltage on surface potential distribution. The experimental setup shown in Fig 3.1-2 was used to deposit charges on insulator surface through corona discharges. The surface potential distributions obtained for different magnitudes of positive and negative dc voltages are shown in the Fig 3.2-1 and Fig 3.2-2. It should be noted that the corona belt was placed approximately at the center of the sample and the charging time was 2 minute. From Fig 3.2-1 and Fig 3.2-2, it can be observed that the potential value at the center of the surface increases with the increase of charging voltage during both positive and negative charging. One can observe that higher charging voltage results in wider spreading of the charge spot. It should be noted that based on these results, ± 7 kV corona charging voltage was selected for further investigations of the effect of time and belt position on the surface potential distribution.

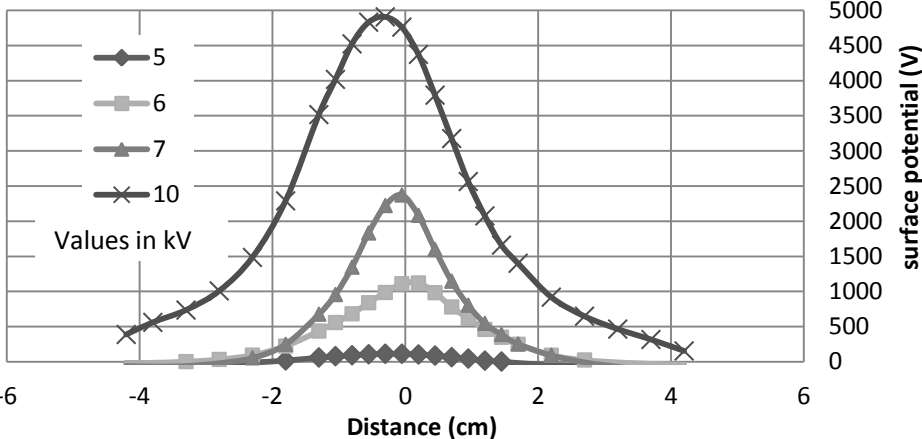


Figure 3.2-1: Potential distribution for 5, 6, 7, 10 kV

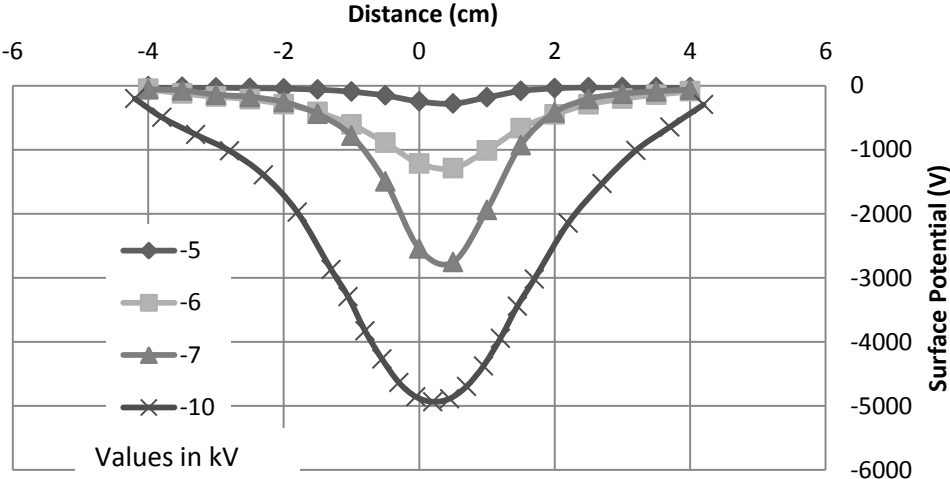


Figure 3.2-2: Potential distribution for -5, -6, -7, -10kV

The potential distribution obtained for time duration of 1, 2 and 3 minutes of the corona charging voltage is shown in the Fig 3.2-3 and Fig 3.2-4. From both the figures, it can be observed that the different time durations for which the sample is charged by corona

doesn't affect the potential distribution significantly and only weak spread of potential along the surface can be observed with increasing time. Similar conclusion has been made in [1], based on the fact that the corona charging during 2 minutes resulted in ~65% of the magnitude of the surface potential as compared to that at 200 minutes (two orders of magnitude longer) charging time.

It should be noted that for further study 2 minutes of the corona charging was used throughout the experimental work.

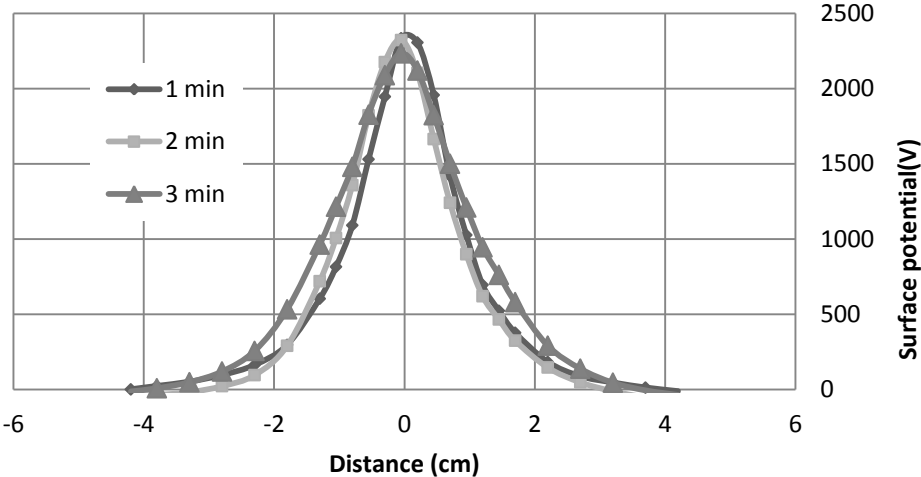


Figure 3.2-3: Potential distribution for 1, 2 and 3 minutes of the positive corona charging

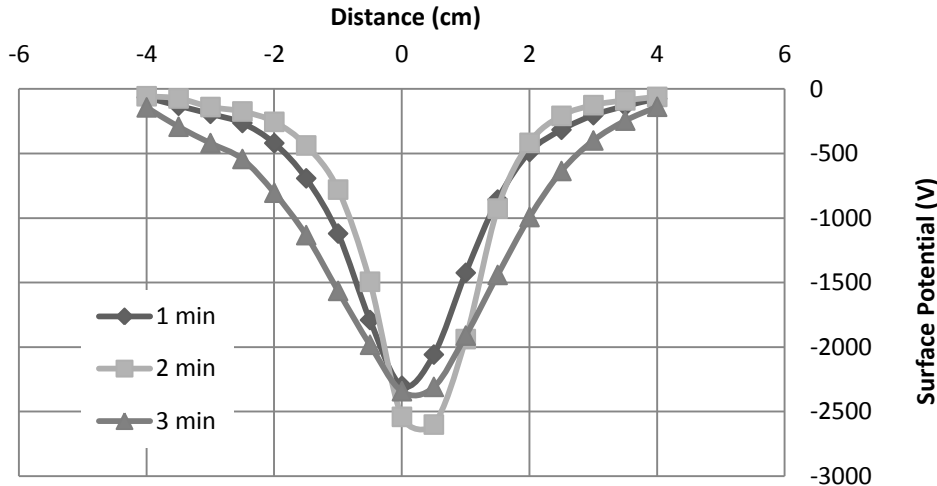


Figure 3.2-4: Potential distribution for 1, 2 and 3 minutes of the negative corona charging

The position variation study was done by placing the corona belt at 1, 2, 3 and 4 cm from the center position for both left and right sides. The potential distribution for left and right side with respect to the center position (marked as 0 distance) of the corona belt is shown in Figs. 3.2-5 – 3.2-8 for both positive and negative voltages respectively.

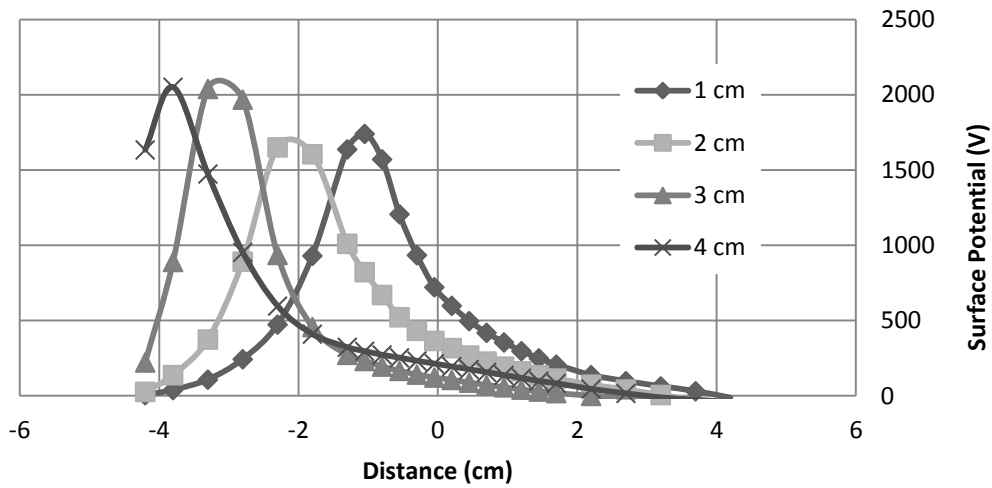


Figure 3.2-5: Potential distribution for position variation (left)

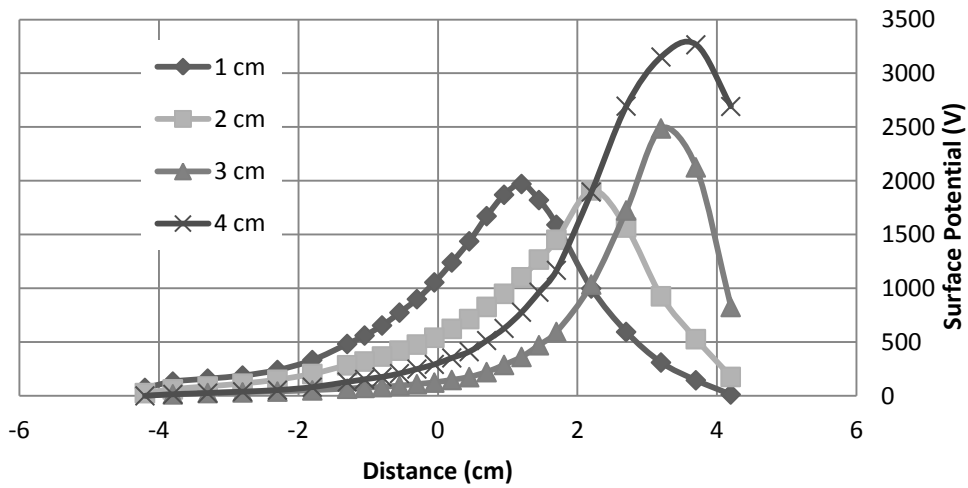
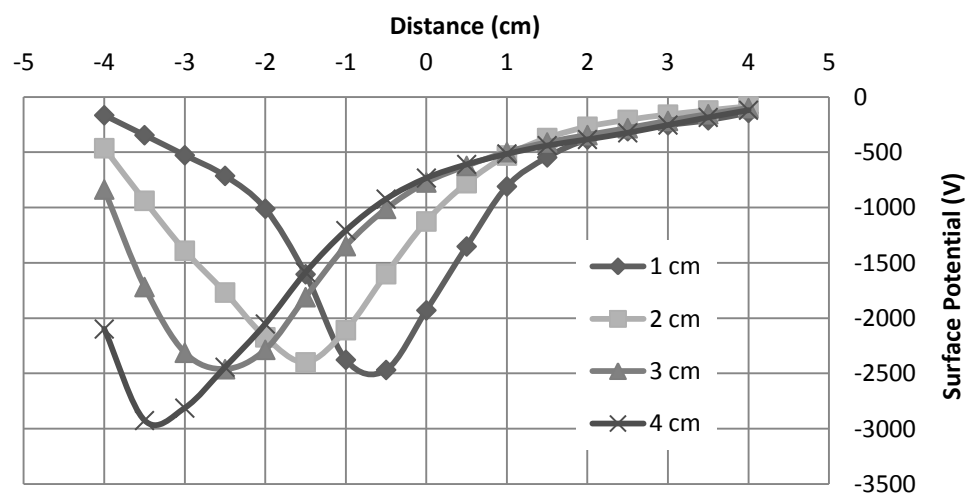


Figure 3.2-6: Potential distribution for position variation (right)



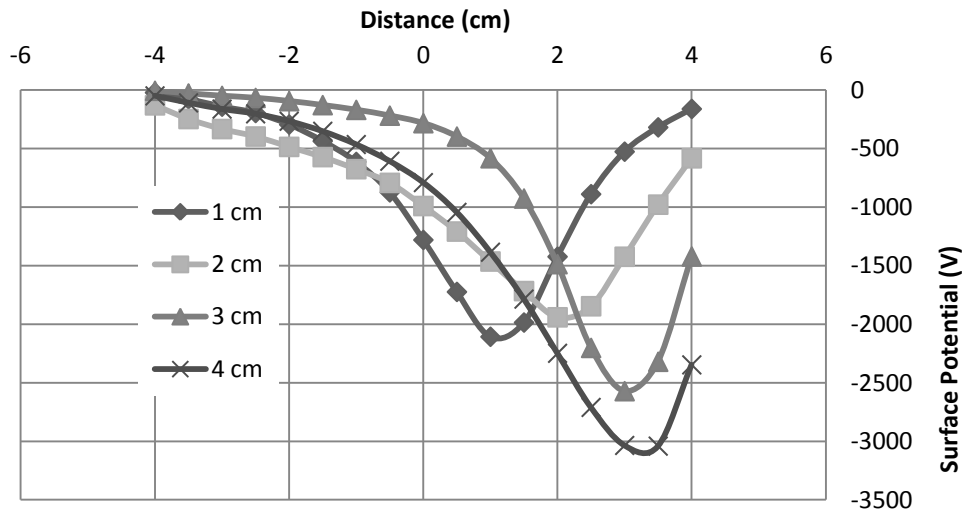


Figure 3.2-8: Potential distribution for position variation (right)

From all the figures it can be observed that the potential distribution at different positions for both the polarities is a shifted version of the potential distribution at the center. Movement of the belt to the left and right give same results due to the symmetry of the electrode arrangement. The placement of corona belt closer to the grounded electrodes increases the intensity of corona discharges as a result of higher field strength, which causes an injection of higher amount of charges from the tip of the needles resulting in higher surface potential magnitudes which is visible in all the figures.

3.3. Experimental results

Different experiments were performed to investigate the surface potential distributions resulted from (i) pre-stressing of the insulator sample, (ii) due to surface charges deposited by preceding flashover, (iii) external corona, and (iv) combine effect of corona discharges and pre-stressing. For the first two cases, the setup shown in Fig 3.1-3 was used and the rate of rise of the voltage was set to 0.83kV/sec.

3.4. Surface potentials due to pre-stressing

Preliminary experiments showed that the flashover voltage of the insulator sample was on the level of -80kV. Therefore, the sample was stressed for 120 sec by applying lower voltages, -72, -60 and -48 kV, and the potential distributions measured at 60 sec after grounding both electrodes of the insulator are shown in Fig 3.4-1. As one can observe, pre-stressing led to quite high potential magnitudes on the surface. However, it appeared to be practically independent on the stressing voltage on the grounded side of the insulator (distance -4 cm). At the same time, a strong increase of the surface potential with the stressing voltage can be seen on the other side close to the electrode, which was connected to the dc voltage supply during energizing. It is notable that the surface potential distributions are practically linear in the regions between the maximum and minimum values and the slopes of the curves are greater at higher stressing voltages. These results are in

agreement with earlier reported observations. Thus in [1], it was shown that for voltage amplitudes of 33.1 kV, 40.4 kV and 45.3 kV, the negative charges are more prominent near the lower electrode and change to positive charges midway on the insulator surface. The dominant character of positive charges with increasing amplitude and always existing accumulation competition between positive and negative charges were also observed.

Based on the presented results, the pre-stressing voltage of -72 kV was used throughout the rest of the experimental work.

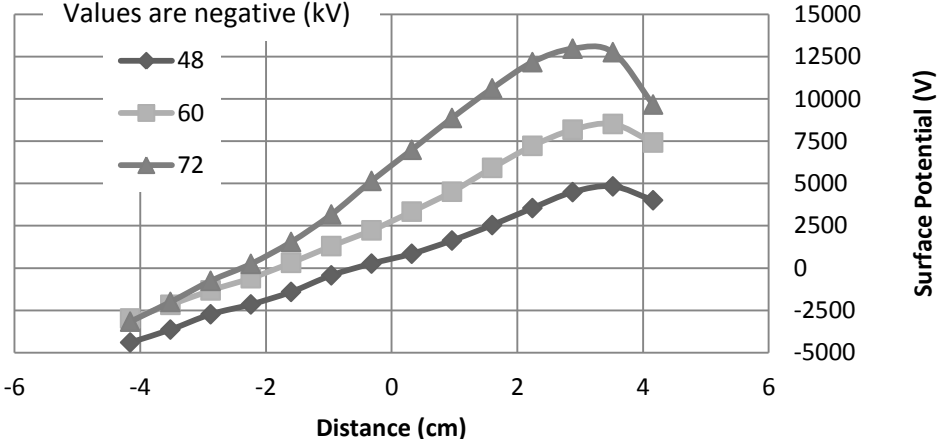


Figure 3.4-1: Surface potential distribution due to pre-stressing. During pre-stressing, the energized electrode was located at 5 cm from the center of the sample.

3.5. Surface potentials due to preceding flashovers

The surface potential distribution measurements, for both clean and initially stressed by -72 kV insulators, were conducted at 60 sec after flashover event. The surface potentials obtained for clean surface at different flashover voltages are shown in the Fig 3.5-1. As one may note, the potential remaining on the surface after flashover was significant reflecting high amount of the deposited charges. In contrast to the case of pre-stressing, the distributions are characterized by two extremas appearing close to the electrodes.

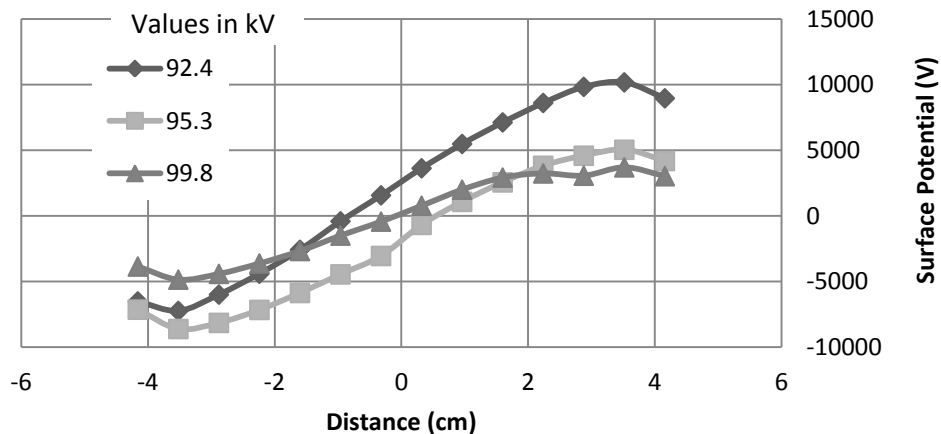


Figure 3.5-1: Surface potential distribution after flashover for clean sample. The magnitudes in the legend are for negative dc flashover voltages.

The measured surface potential distributions for the second case, where the sample was first stressed by applying -72 kV for 120 sec and then the voltage was raised up to flashover, are shown in the Fig 3.5-2.

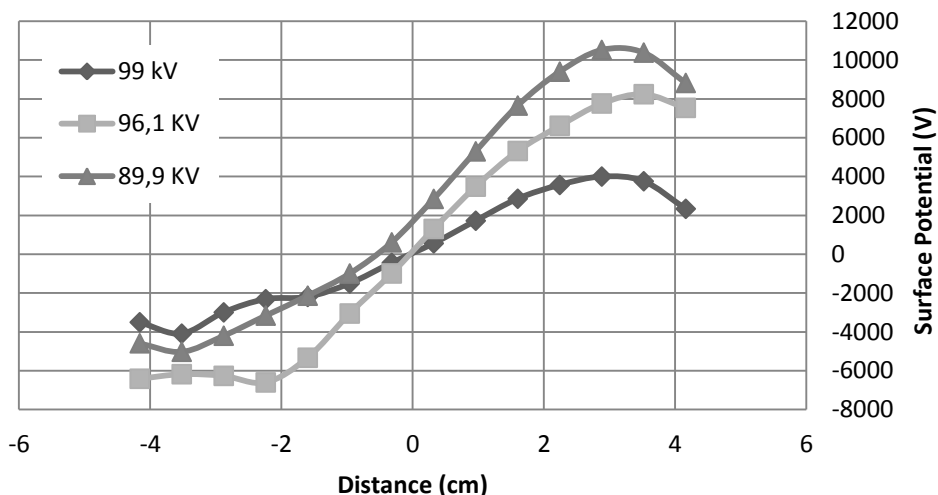


Figure 3.5-2: Surface potential distribution after flashover for stressed (72kV) sample. The magnitudes in the legend are for negative dc flashover voltages.

Comparing Figures 3.5-1 and 3.5-2, one may conclude that the surface potential distributions are similar for both the cases meaning that different flashover events deposit their own charges on the surface and this doesn't depend on the initial conditions, i.e. whether the sample surface was clean of charges or it was pre-stressed by some voltages.

3.6. Surface potentials due to external corona

Different experiments were performed to investigate effects of the position of corona belt and discharge intensity on characteristics of potential distribution along the surface. Here, the results corresponding to central location of the corona belt are presented. The surface potential distributions measured for 10, 12, 15, 18 and 20 kV charging voltages are shown in Fig 3.6-1 and Fig 3.6-2 for positive and negative corona, respectively.

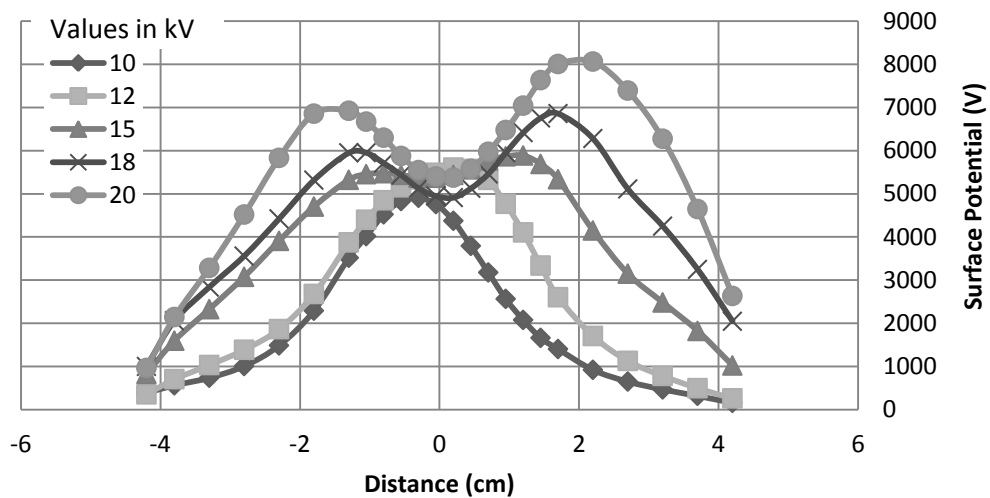


Figure 3.6-1: Potential distribution for positive voltages

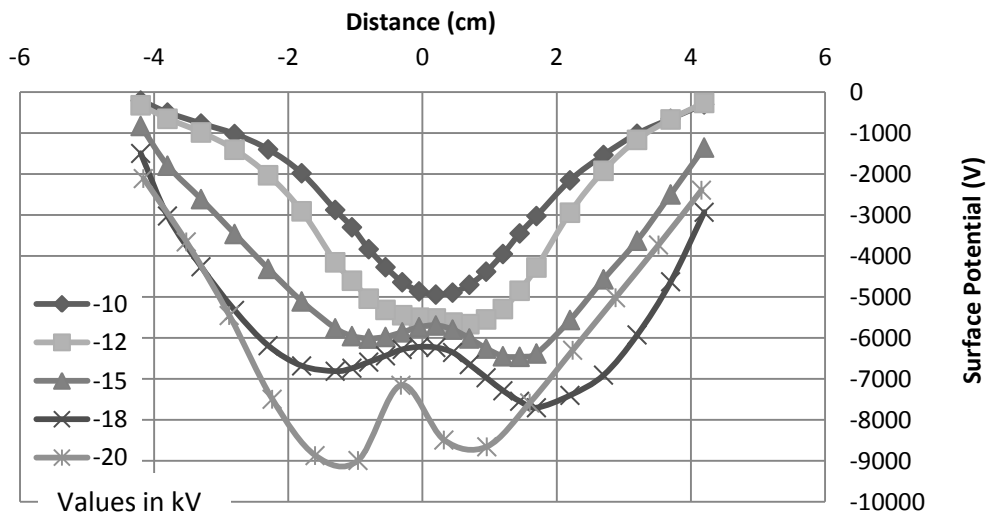


Figure 3.6-2: Potential distribution for negative voltages

As it can be seen from the graphs, the potential distributions obtained for different polarities of the corona discharges are very similar at corresponding voltages. Thus, the potential distributions for ± 10 and ± 12 kV corona charging voltage are bell shaped, however, they are transformed into saddle shaped as the voltage approaches ± 15 kV. The saddle becomes even more prominent for ± 18 and ± 20 kV corona charging voltages. The conversion from bell to saddle shape may be due to back discharges and it is also observed and documented by several authors [22, 23].

It should be noted that even though the experiments for each voltage were repeated three times, only one curve for each voltage is shown here. The graphs for the potential distributions at different positions of the corona belt and repeatability analysis are given in the appendix A1.

3.7. Surface potentials due to pre-stressing and external corona

To investigate the combined effect, the insulator sample was first stressed by -72 kV for 120 sec and then exposed to corona discharges at different voltages and different positions for 120 sec. The time duration between the pre-stressing and application of corona discharges was kept at 60 sec that was needed to install the corona belt. The potential distributions for ± 10 kV and ± 15 kV corona charging voltages and central position of the corona belt with pre-stressed sample are shown in Fig 3.7-1 and Fig 3.7-2 for positive and negative polarities, respectively. Potential distributions for other positions of the corona belt and pre-stressing voltages are given in the appendix A2.

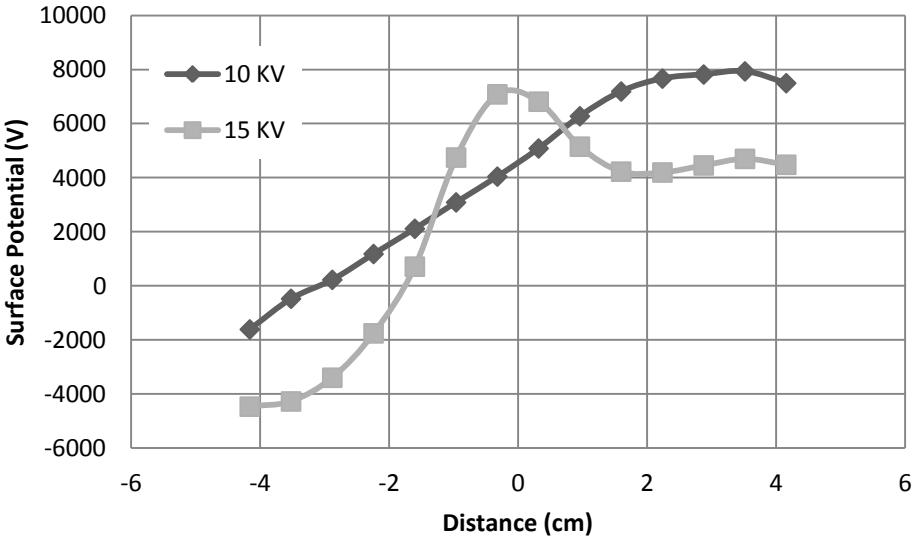


Figure 3.7-1: Surface potential distributions for the combined charging: -72kV pre-stressing and positive external corona

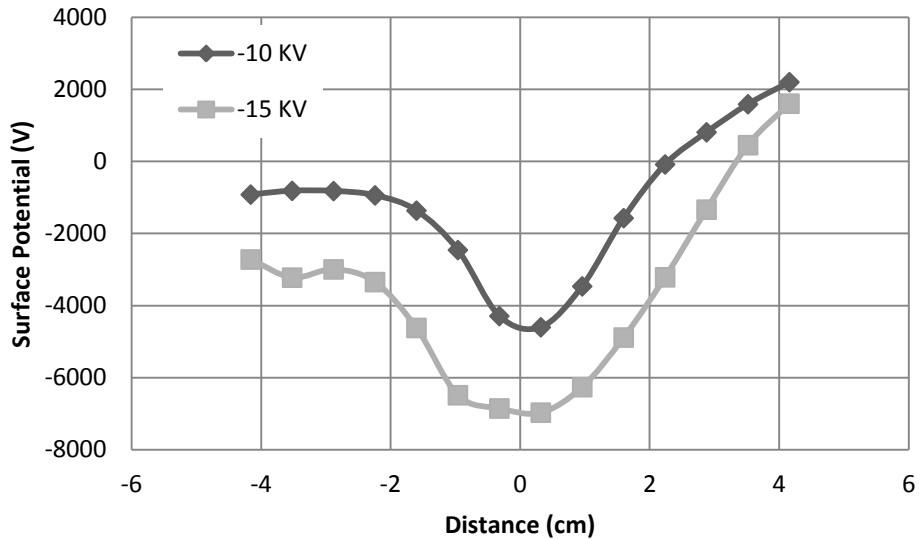


Figure 3.7-2: Surface potential distributions for combined charging: -72kV pre-stressing and negative external corona

From Fig 3.7-1 it can be observed that the surface potential profile originally caused by -72 kV stressing was not significantly affected by superimposing 10 kV positive corona charging voltage, while a slight change can be observed for 15 kV. In case of negative corona charging voltages, shown in figure 3.7-2, both the voltage levels (-10kV and -15kV) caused a change in the surface potential profile due to -72 kV. The reason may be due to the same nature of the voltage polarity for both the pre-stressing and external corona charging.

3.8. Surface potentials due to preceding flashover and external corona

In this case, the voltage from the dc generator was applied first to get the flashover and then the sample was exposed to corona discharges for 120 sec. The time duration between the flashover and corona discharges was kept 60 sec needed to install the corona belt. The potential distributions for ± 10 kV, ± 15 kV and ± 20 kV corona charging voltages and central location of the corona belt with charges from the preceding flashovers are shown in Figs 3.8-1 and 3.8-2. The surface potential distributions for other positions of the corona belt are given in appendix A3.

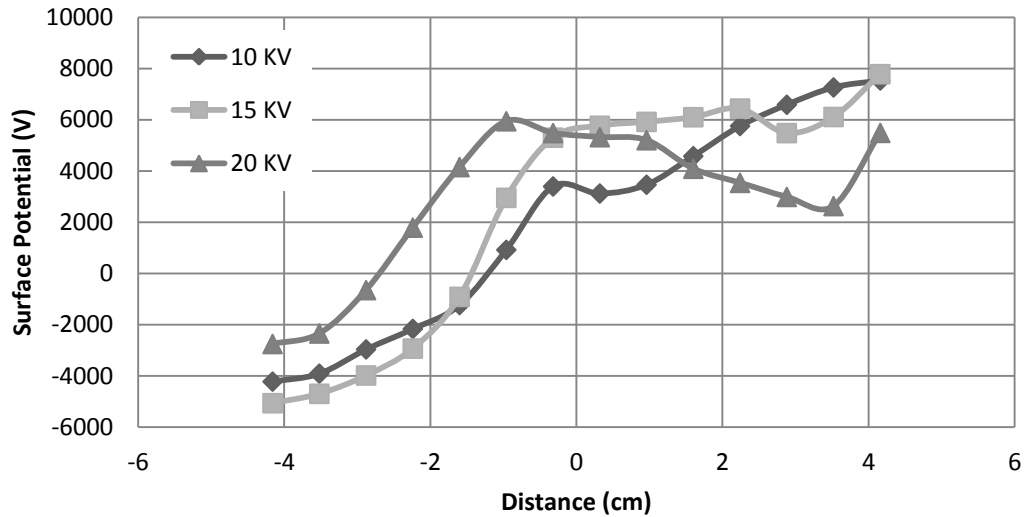


Figure 3.8-1: Surface potential distributions for combine charging: flashover (negative) and positive corona discharges.

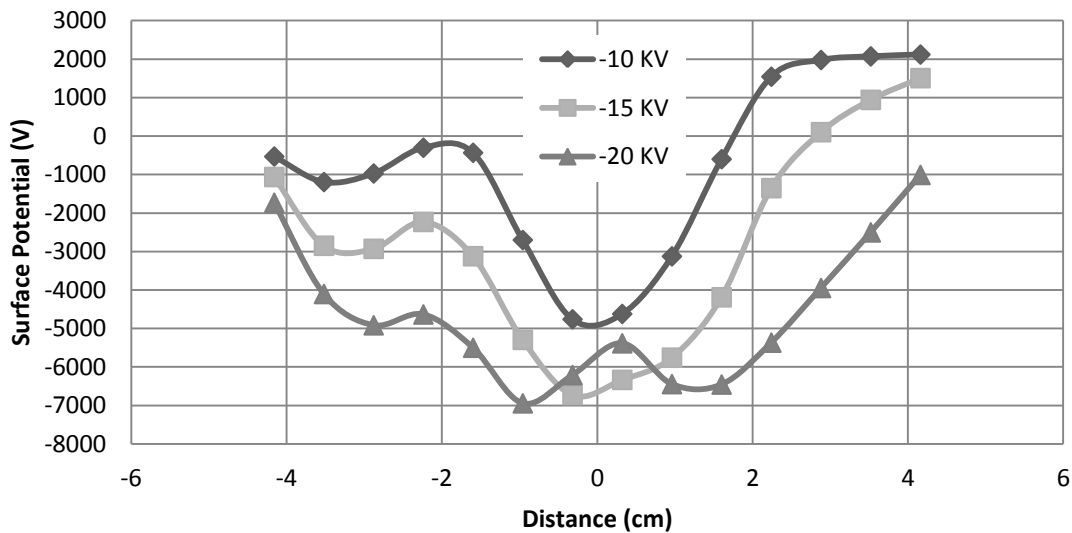


Figure 3.8-2: Surface potential distributions for combine charging: flashover (negative) and negative corona discharges.

From Fig 3.8-1 it can be observed that the positive corona charging voltages don't have a significant effect on the surface potential originally caused by different flashover events. In case of negative corona charging voltages, shown in Fig 3.8-2, a significant change can be seen in the surface potential profile originally caused by the different flashover events. The reason may be due to the same nature of the voltage polarity for both the flashover and external corona charging.

3.9. Surface potential decay measurements and interpretation

Measurement of surface potential decay on corona charged polymeric materials is a powerful tool to characterize insulating materials, charging methods and various electrical properties such as charge transport, trapping/detrapping, neutralization and recombination.

Surface potential decay measurements can be used as a technique to diagnose the dielectric properties. Over the last couple of decades, potential decay measurements have been widely published and various models have been proposed to describe electrical properties such as charge transport within the material and charge spreading over surfaces etc [14, 15, 24, 25]. The surface potential decay curves have been presented in different formats such as “V vs. time” and “log V vs. log time” to suggest a quantitative interpretation of the initial stages of the decay and also to discuss the cross-over phenomena.

The measured surface potential decay obtained after charging the insulator surface by corona with 7 kV is shown in Fig 3.9-1 as a plot of “V vs. time”. Similar decay characteristics obtained under different scenarios are shown in appendices A4, A5 and A6. The surface potential was measured at the center of the sample by means of electrostatic probe and the measuring system was described in section 3.1. The surface potential decay in our experimental setup with grounded surface (metal insulator interface) and a free surface (air insulator interface) is a consequence of various physical phenomena’s [24]. The initial stage of surface potential decay is related to the amount of charge deposited on the insulator. The higher the initial potential is, the higher is the rate of decay during initial stage. This may be due to the higher energy of charged particles that may lead to a higher initial capability of surface conduction. The important point here is to note that a fast potential decay occurs only when the electric field across the sample exceeds a certain value [14]. The part of the curve corresponding to the longer time is smoother and the decay rate is lower. The reason is due to the lower potential energy possessed by the charge carriers and, as a consequence, charge spreading over the surface becomes less intensive and slow decay mechanisms (like bulk conduction and neutralization) are dominant.

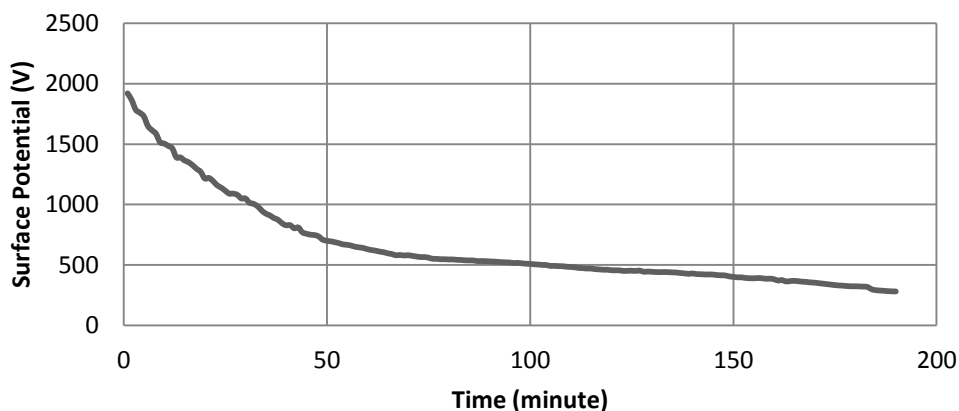


Figure 3.9-1: Surface potential decay measurement (V vs. time)

The surface potential cross-over phenomena was first reported by *Ieda et al* in 1967. The observed cross-over phenomena was interpreted as “initially the surface potential of a sample charged to high-potential decays more rapidly than one charged to a lower potential” [14]. Similar behavior was observed in the present experiments and it is illustrated in Fig 3.9-2 as log V vs. log time plot.

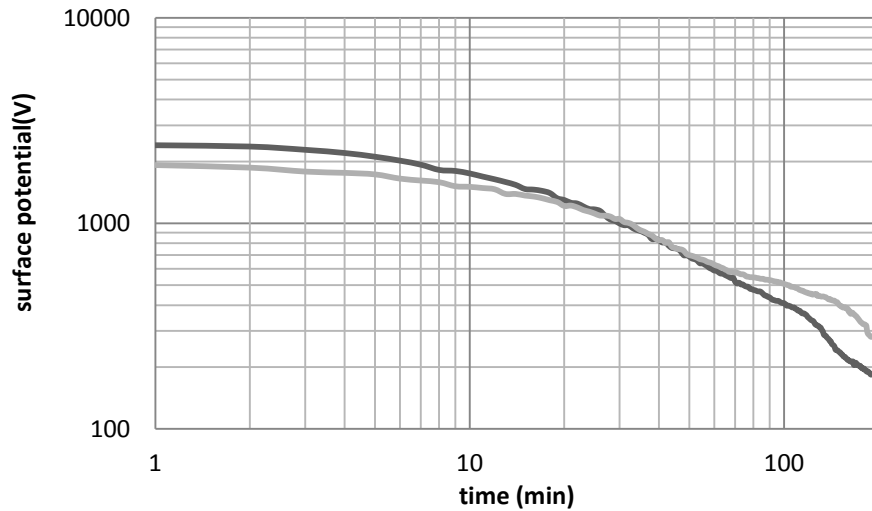


Figure 3.9-2: Surface potential decay

Most of the literature interprets the time decay of the surface potential in terms of surface conduction, charge injection and volume polarization. The recent theories on surface potential decay are based on the hypothesis of charge injection into the bulk of the material (bulk conduction) accompanied by slow process of volume polarization [14]. Some of the authors also suggest that potential decay may not be caused by charge injection into the bulk rather neutralization caused by the compensation of the arrival of charges of opposite polarity onto the sample surface. Chinaglia et al. has confirmed the arrival of the charges of opposite polarity [13].

To explain the cross-over phenomena and initial stage of decay various models have been proposed and certain assumptions and hypothesis have been documented such as partial injection and time dependent injection.

CHAPTER 4: SIMULATION OF SURFACE CHARGING OF POLYMERIC INSULATORS

This chapter discusses computer simulations of surface charge distributions deduced from the surface potentials obtained in the laboratory experiments.

4.1. Model description

In the experimental setup, the potential was measured along the surface of the polymeric insulator after applying various charging conditions. In order to get an actual idea on how the charges are accumulated on the surface and to see how the charge distribution looks like, a model was developed in Comsol multiphysics 3.5a which is based on finite elements method. The 3D geometry of the electrode system including the grounded floor of the lab was drawn with the exact dimensions. A schematic diagram of the whole geometry including boundary conditions is shown in Figure 4.1-1. To limit the computational domain, a box with dimensions of $2 \times 2 \times 1.6 \text{ m}^3$ was used. Various other parts, which play insignificant role in the field calculations, were neglected in the model to reduce the computational complexity. These parts were the robot arm, belt supporting legs, grounding wires, the base, etc. Although the measuring probe affects the electric field and potential distribution around the sample, the probe effect was neglected in this study. Thus, one can assume that the measured potential is the actual potential on the surface irrespectively of the presence of probe. The Electric field in the entire domain was calculated by solving Laplace equation available in the Electrostatics application mode.

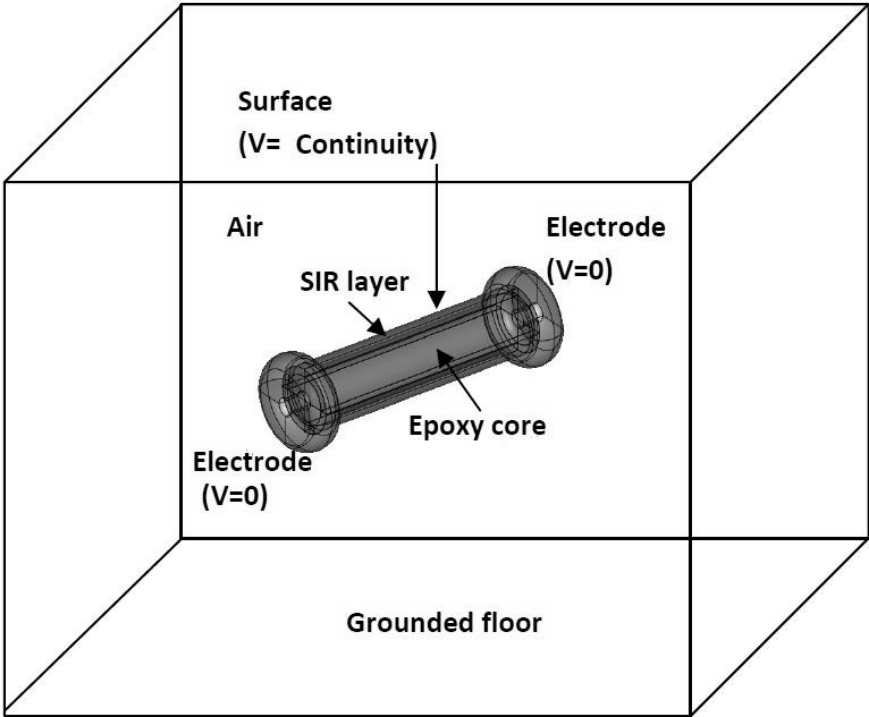


Figure 4.1-1: Representation of the insulator with electrodes in Comsol Multiphysics.

Model parameters:

Insulator length 13.2 cm (including electrodes)
Insulator diameter 8.5 cm (Inner diameter 8 cm, outer diameter 8.5 cm)

The relative dielectric permittivity for the silicone rubber layer $\epsilon_r=3.5$ and for the fiber reinforced epoxy core $\epsilon_r=4$ [26]. The box surrounding the insulator contains air $\epsilon_r=1$.

Mesh

In these simulations, the default element type was Lagrange- quadratic and the surface potential data acquired from the experiments were used as a boundary condition in the simulation. The parameters of the generated computational mesh are given in the table and the meshing of the insulator is shown in the Fig. 4.1-2.

Mesh Statistics

Number of degrees of freedom	45175
Number of mesh points	6254
Number of elements	34102
Tetrahedral	34102
Prism	0
Hexahedral	0
Number of boundary elements	4236
Triangular	4236
Quadrilateral	0
Number of edge elements	632
Number of vertex elements	78
Minimum element quality	0.224
Element volume ratio	0

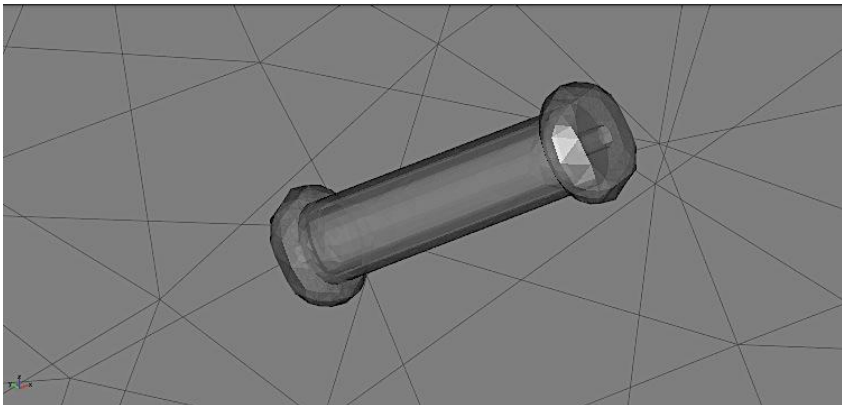


Figure 4.1-2: Meshing

4.2. Results

During the laboratory experiments, surface potential data was acquired by means of Kelvin probe connected to an electrostatic voltmeter. Upon completion of the charging, both the electrodes were grounded and the surface potential measurements were carried as described in chapter 3. In the model, the measured surface potential distribution was used as the boundary condition for the insulator surface. The problem was solved and the surface charge distribution was obtained as the normal component of the displacement vector represented by the variable “nD_emes” available in the post processing section (“Domain plot parameters”). Some of the typical results are presented in this section.

4.2.1 Charging by external corona

The first case presented here shows the surface charge density due to corona charging of a grounded insulator sample. The following Figure 4.2-1 shows the charge accumulation on the surface due to applying ± 7 kV to the corona belt. Figure 4.2-2 is for the same configuration but for ± 20 kV corona voltage.

It is evident from the figures that surface charge distributions follow the surface potential profiles. In the region of higher potentials, charges are also gathered in higher quantity. From Figure 4.2-2, it can be seen that opposite charges are accumulated right under the belt needles at the centre, possibly due to back discharges. Possibly this causes the saddle shape to appear in the potential distributions of figures 3.6-1 and 3.6-2.

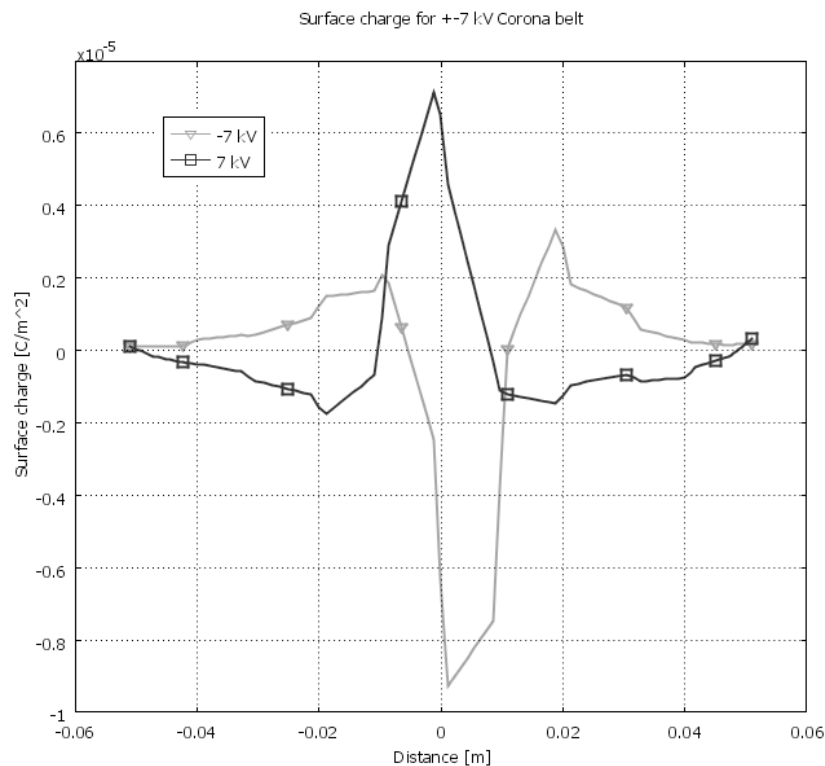


Figure 4.2-1: Surface charge for ± 7 kV Corona belt

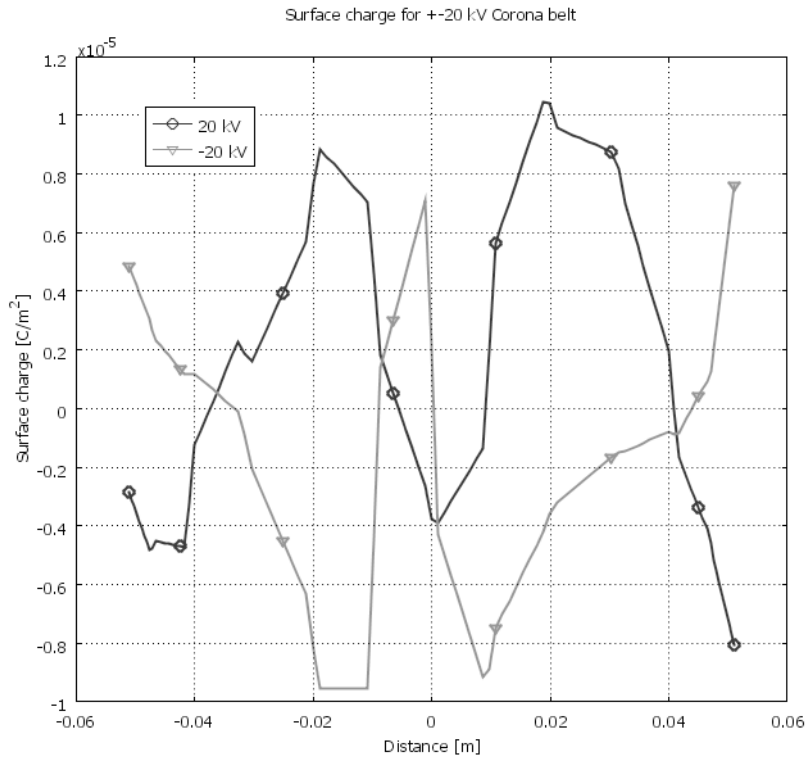


Figure 4.2-2: Surface charge for ± 20 kV Corona belt

4.2.2 Pre-stressing only

The calculated surface charge density distributions resulting due to pre-stressing with -48, -60 and -72 kV are shown in Figure 4.2-3. As it can be seen, most of the sample is positively charged. Negative charges appear close to the negative electrode and positive charges gather close to the positive electrode.

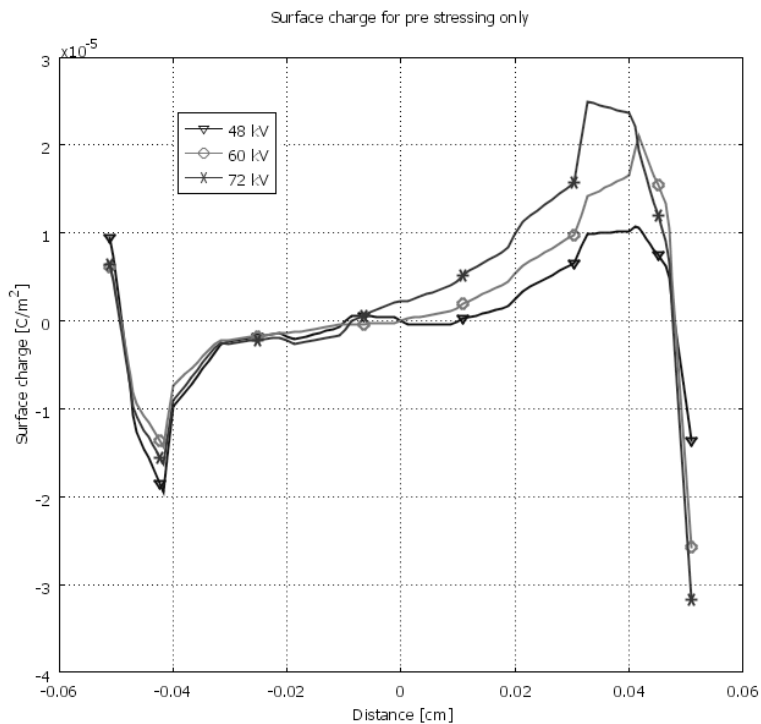


Figure 4.2-3: Surface charges on pre-stressed insulator

4.2.3 Surface charges due to pre stressing and external corona

The figure 4.2-4 shows the results obtained for the combined effect of the pre-stressing at -72 kV and external corona at ± 15 kV. As it can be seen, the surface charge magnitude at the center is higher in case of positive corona than the negative one.

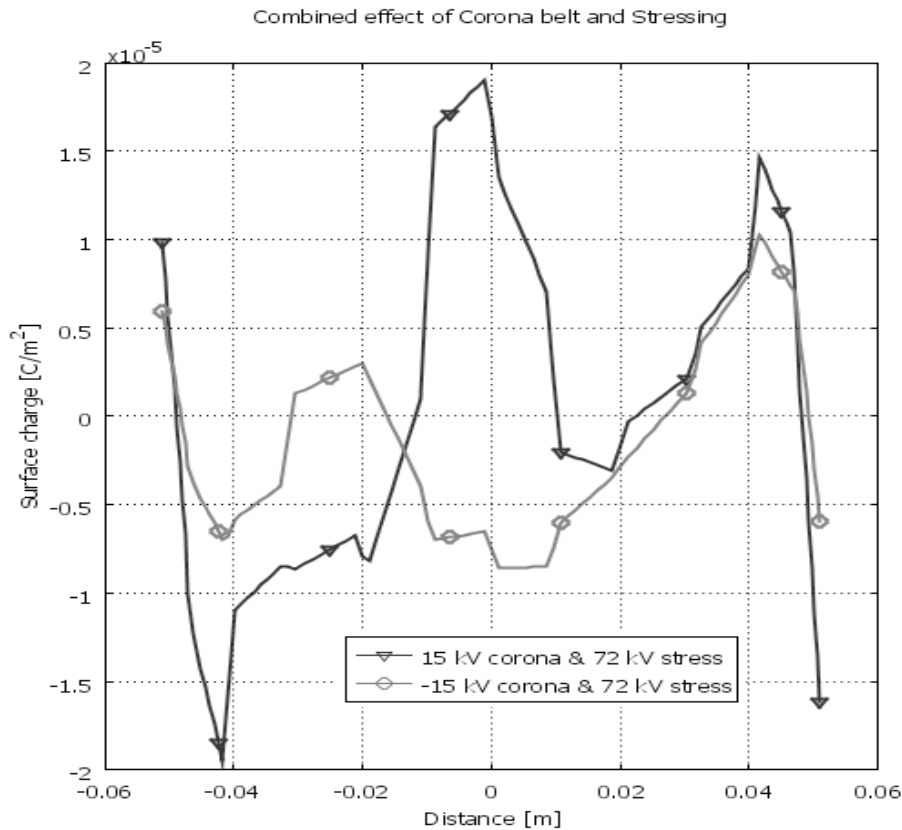


Figure 4.2-4: Combined effect of pre-stressing and corona

These set of simulation results show that, the model developed in comsol for converting surface potential distribution to surface charge distribution, is capable of doing such function. Although the effects of the scanning probe was not implemented, this simulation model is capable of producing results which are very good approximation of the actual distributions of charges on the insulator surface. However this opens opportunities for further studies related to calculation of exact charge distributions.

CHAPTER 5: EFFECT OF SURFACE CHARGES ON DC FLASHOVER CHARACTERISTICS OF CYLINDRICAL POLYMERIC INSULATORS

This chapter summarizes the dc flashover characteristics of the cylindrical polymeric insulator in presence of surface charges. The effect of various parameters related to surface charging such as voltage magnitude, polarity and position of the corona belt on the flashover characteristics are summarized.

5.1. Experiment setup and procedure

The experimental set up for obtaining dc flashover characteristics of the insulator was similar to that used for pre-stressing of the insulator and it is shown in Fig 3.1-6 (see also related text).

The procedure for measuring dc flashover characteristics of polymeric insulators is not well established. General guidelines for dc withstand tests are given in [27], where time duration of the applied voltage, its levels, temporary overloading, etc. are specified and withstand performance is defined in terms of the duration of the applied voltages for various components from several hours to several thousand hours. At present, no mandatory IEC standards are defined for dc flashover procedure in terms of rate of rise of the applied voltage. According to the IEC 60060-1 standard, the voltage rise time during disruptive discharge test should be on the level of 2% of the expected flashover voltage per second. Therefore, the rate of rise of applied voltage 0.83kV/sec was chosen in the experiments.

The tests were performed in an indoor high voltage laboratory where the conditions were closed to the standard atmospheric conditions, so the atmospheric correction factor was close to unity.

The dc flashover tests were conducted for different scenarios and the related experimental procedures will be presented in each section below in details.

5.2. Experimental results

Preliminary measurements were performed to investigate the effect of cleaning and pre-stressing of the insulator on the flashover voltages. According to the observations from the preliminary studies, the experimental work was focused on several scenarios of the conditions for the charging of the insulator. The flashover tests for each scenario were performed 6 - 10 times to check the repeatability and avoid any ambiguity. Average flashover values and ranges of their variations are presented below whereas exact flashover values for each trail are given in appendix B.

5.2.1 Preliminary studies

The flashover test without surface charging was performed to obtain a reference breakdown voltage for the insulator with clean surface. Before performing the test sample surface was cleaned using a solvent iso-propanol and surface potentials were measured as described in

section 3.1 to ensure that there were no significant charges left on the surface. The breakdown voltages were recorded for each test and the average, maximum and minimum breakdown voltages were found to be -87.4 kV, >-100 kV, and -79.7 kV.

5.2.2 Flashover voltage with charges from previous flashover event

The test was carried to obtain flashover voltages in presence of charges left on the surface after preceding flashover. The experimental procedure for this kind of test was as follows:

1. Clean the insulator surface
2. Measure surface potentials to ensure that the surface has no significant charges
3. Pre-stresses the insulator to a certain voltage and keeps it for 120 sec
4. Wait 60 sec and apply the voltage to get the breakdown
5. Repeat step (4) 6 times

Different pre-stressing voltages were applied to get different initial flashover voltages and, hence, different charge distributions after the first flashover event. The results are shown in Fig 5.2-1, where the error bars represent the range of the flashover values at each pre-stressing voltage. The values shown on the top of each error bar represents the pre-stressing voltage. The middle marked point on each error bar represents the average breakdown voltage. The horizontal axis represents the initial breakdown voltage level, which corresponds to a particular pre-stressing condition. The horizontal line intersecting each error bar represents the total average breakdown voltage and it is calculated as the average of the averaged values for each error bar.

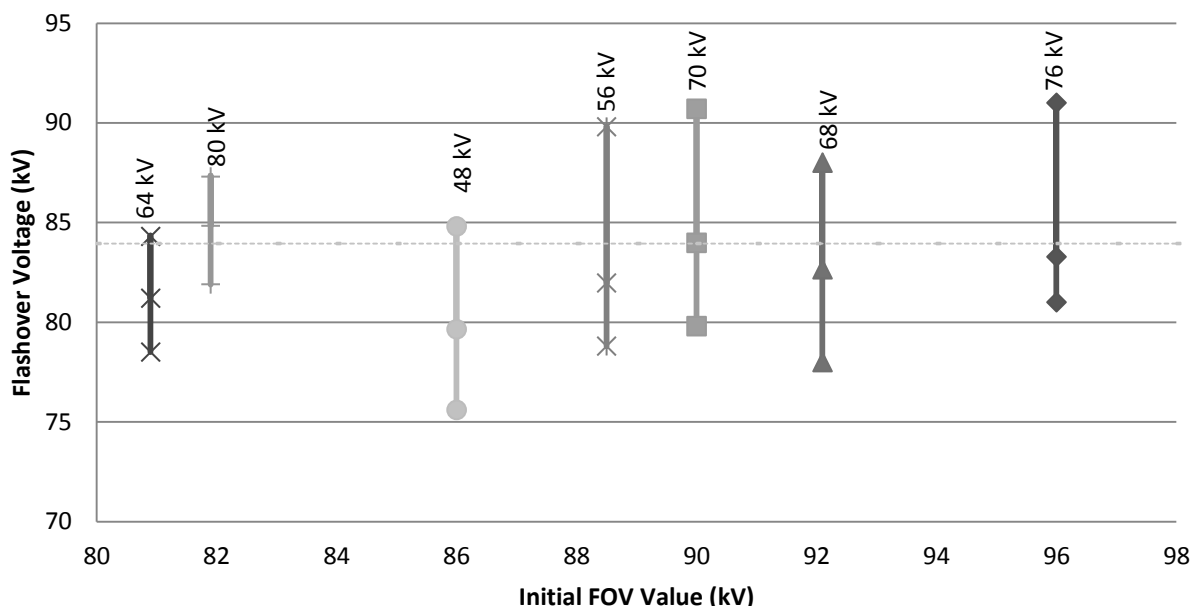


Figure 5.2-1: Magnitudes of the flashover voltages with charges from preceding flashover

From Fig 5.2-1, one may conclude that no matter whatever is the pre-stressing voltage and the initial breakdown voltage, the rest of the breakdown voltages lay almost within the same range. It can also be observed that no matter what is the amount of charges left from the

previous flashover, the total averaged breakdown voltage and the average breakdown voltage marked on each error bar remain almost constant. To justify the previous explanation and to show the trend of breakdown voltages at a given pre-stressed condition (pre-stressing of -72 kV was applied for 2 min before the first flashover event), a histogram is shown in Fig 5.2-2.

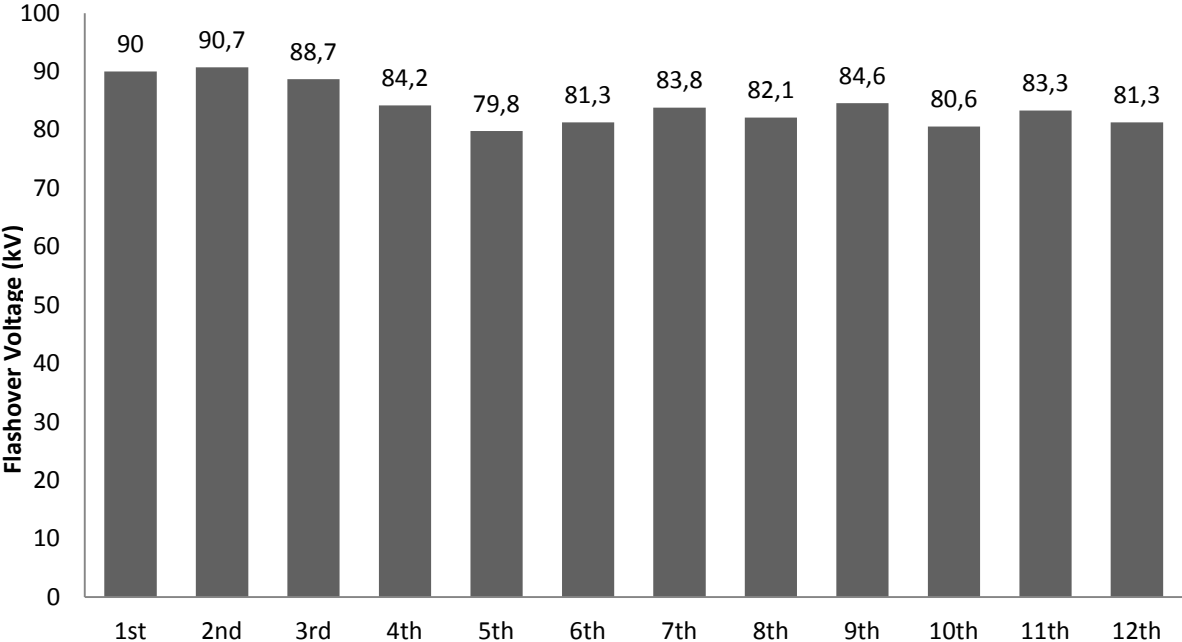


Figure 5.2-2: Flashover voltages at a given pre-stress condition (note that the actual values are negative)

5.2.3 Flashover voltage with pre-stressed sample

To identify the effect of charges from pre-stressing, the flashover test was carried out according to the following procedure:

1. Clean the surface
2. Measure the surface potential to ensure that the surface has no significant charges
3. Stresses the insulator by applying a certain voltage for 120 sec
4. Wait 60 sec and apply the voltage form dc generator up to flashover
5. Note the breakdown voltage and carry out all the steps again.

The experiment for each pre-stressing voltage was repeated 6 times and the flashover values are shown in the Fig 5.2-3. The error bars represent the range of the flashover values at each pre-stressing voltage. The horizontal axis represents the pre-stressing voltage and the vertical axis represents the flashover voltages.

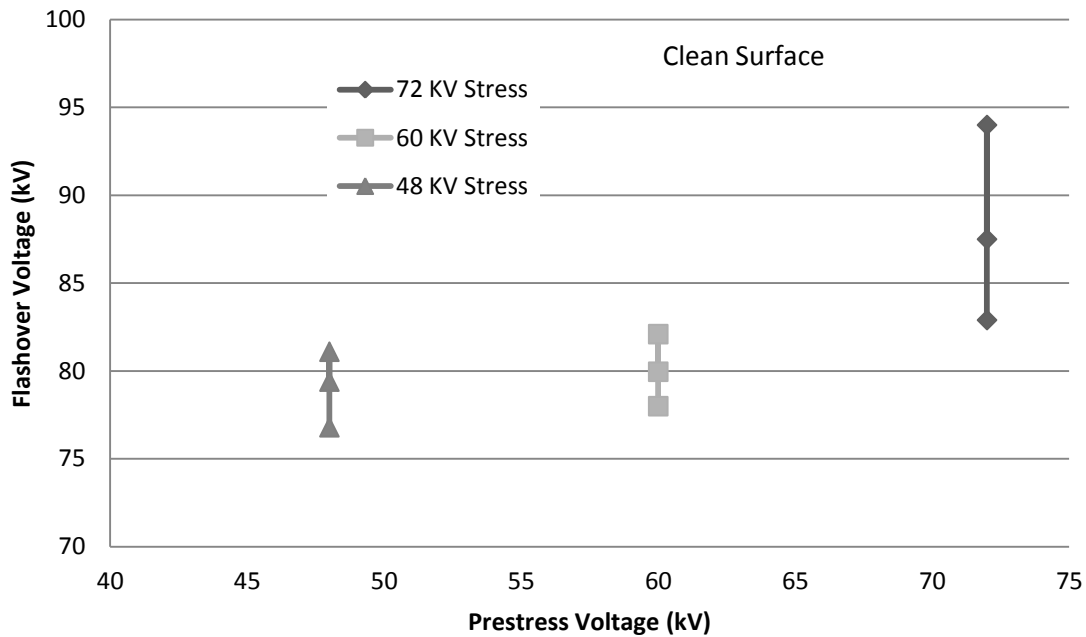


Figure 5.2-3: Flashover voltages at different pre-stressing voltages (note that the actual values are negative)

As it can be observed, the higher the pre-stressing voltage is the higher is the flashover voltage. One can also note that the average breakdown voltage marked on each error bar also increases with the pre-stressing voltage. The reason may be due to the fact that higher pre-stressing deposit higher amount of negative charges resulting in a higher negative dc breakdown voltage.

5.2.4 Measurement of flashover voltage without corona charging

To compare the flashover voltages obtained under different scenarios without corona charging, corresponding experimental results are shown in the Fig 5.2-4. Conditions for each test are given in the legend. In case of pre-stressing with -72 kV both initially cleaned and uncleaned surfaces were considered. The effect of charges from the preceding flashover on the breakdown voltages can be related to presence of charges appearing from two different flashover events, whose flashover voltages are given in the legend.

One can observe that the different charging conditions result in a different range of flashover voltages. Also it can be observed that cleaning the surface results in higher statistical variations. When surface was not initially cleaned, statistical variation lies in a narrow range. Results shown in Fig 5.2-4 can be used as reference values for the results obtained with corona charging presented below.

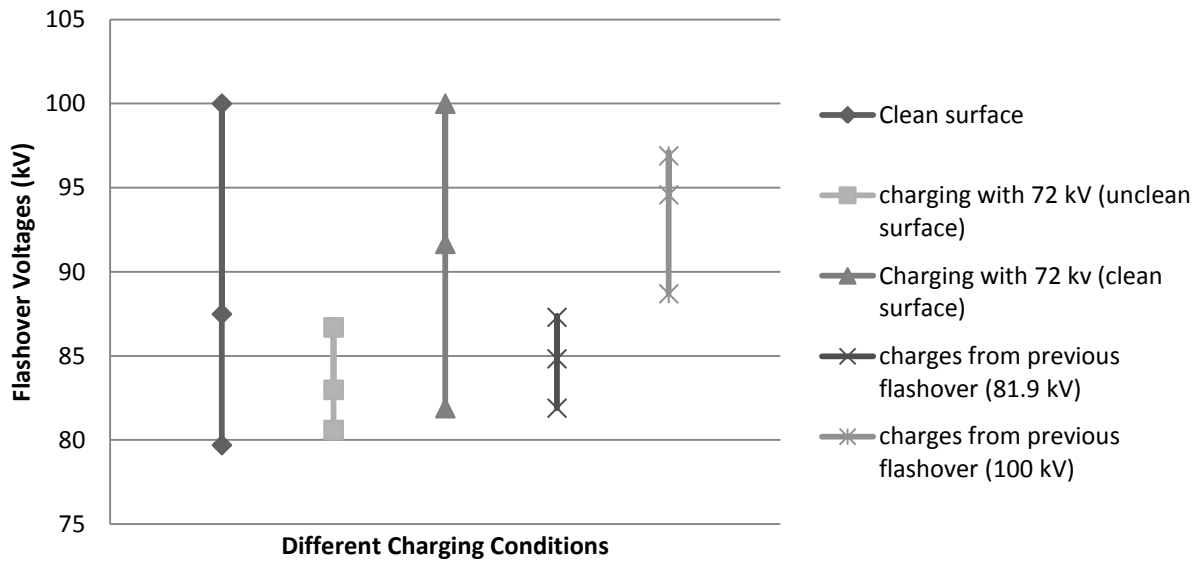


Figure 5.2-4: Flashover voltages without corona charging (note that the actual values are negative)

5.3. Flashover voltages in presence of charges deposited by external corona

To see the effect of surface charges deposited by coronas on the flashover voltages, three scenarios were taken into consideration.

5.3.1 Flashover voltages with charges from preceding flashover and corona

As discussed in section 5.2.2, charges from previous flashovers do not affect significantly the conditions for the next flashover. The results presented in this section were obtained for the case when additional surface charges were generated by external corona. The experimental procedure included the following steps:

1. Apply the voltage from dc generator to get first flashover
2. Set the corona belt within 60 sec
3. Apply corona charging voltage for 120 sec
4. Wait 60 sec
5. Apply the voltage from the dc generator up to flashover
6. Discard the flashover value obtained in the first step and repeat all the steps (excluding the first one) to get the next flashover value.

The experiment was performed for both polarities of the corona discharge, different magnitudes of corona charging voltages and different positions of the corona belt. The experimental results are shown in the Fig 5.3-1.

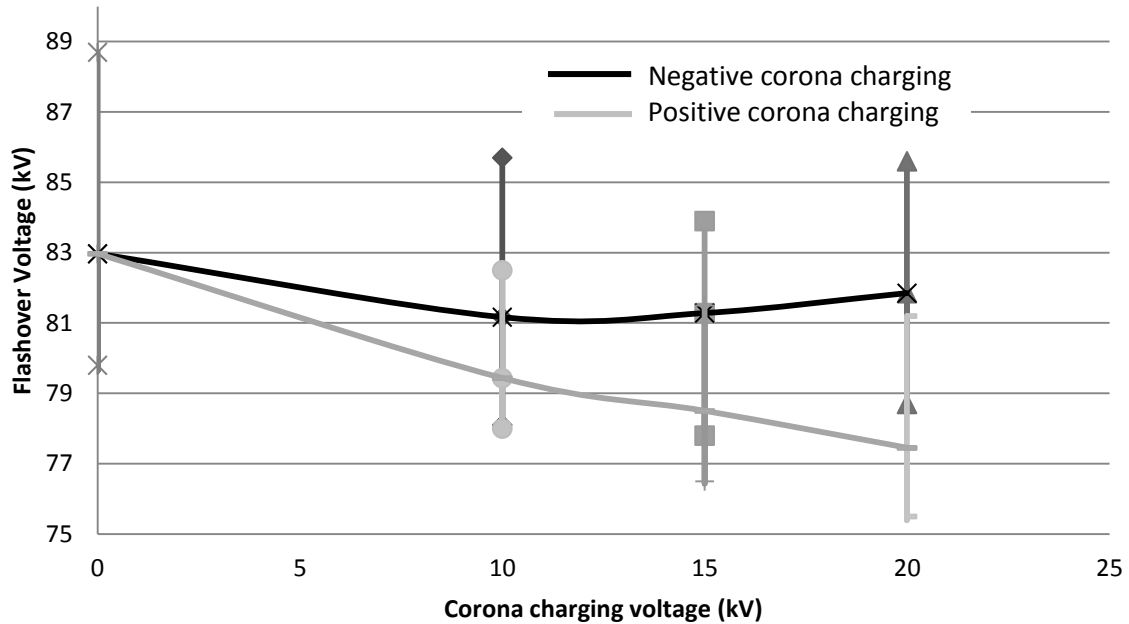


Figure 5.3-1: Flashover voltages with charges from both corona and previous flashover (note that the actual values of the flashover voltages are negative)

In the figure, the horizontal axis represents the magnitudes of the corona charging voltages for both polarities while the vertical axis represents the flashover voltages. The reference shown in the Fig 5.3-1 at zero charging voltage represents the range of flashover voltages with no charges from corona but in presence of charges from preceding flashover. The error bars marked with different symbols represent the range of flashover voltages for both negative and positive corona charging voltages. From Fig 5.3-1, one may note that the negative corona charging produces practically no effect on the average flashover voltages. In case of positive corona, a reduction of the average breakdown voltages can be observed with increasing charging voltages.

5.3.2 Flashover voltage with charges from pre-stressing and external corona

The effect of charges from pre-stressing was discussed in section 5.2.3. To see the combine effect of the charges from both pre-stressing and corona on flashover voltages, the experiment was performed according to the following steps:

1. Clean the surface
2. Measure the surface potential to ensure that the surface has no significant charges
3. Pre-stresses the insulator by a certain voltage for 120 sec
4. Set the corona belt within 60 sec
5. Apply corona charging voltage for 120 sec
6. Wait 60 sec
7. Apply the voltage from the dc generator again to get flashover
8. Note the flashover value and repeat all the steps 10 times.

The experiment was performed for both the polarities, different magnitudes of corona charging voltages and different positions of the corona belt. The experimental results are shown in the Fig 5.3-2.

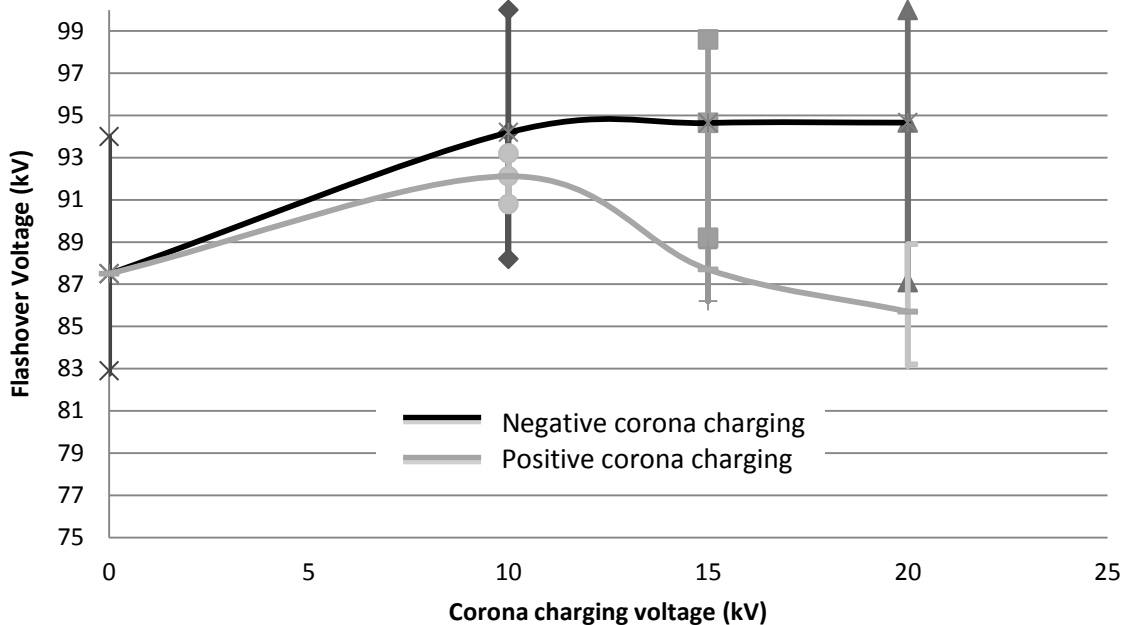


Figure 5.3-2: Flashover voltages with charges pre-stressing and corona (note that the actual values of the flashover voltages are negative)

The reference shown in Fig 5.3-2 at zero charging voltage represents the range of flashover voltages obtained with no charges from corona but in presence of charges deposited during pre-stressing. From the figure, one can note that corona charging weakly affects the average flashover voltages at both polarities.

5.3.3 Flashover voltage with charges from corona only

To see the effect of charges from corona only on the breakdown voltages, the experimental work was carried out according to the following steps:

1. Clean the surface
2. Measure the surface potential to ensure that the surface has no significant charges
3. Set the corona belt and apply corona charging voltage for 120 sec
4. Wait 60 sec
5. Apply the voltage from the dc generator to get the breakdown voltage
6. Repeat all the steps 10 times

The experiment was performed for both the polarities, different magnitudes of corona charging voltages and different positions of the corona belt. The experimental results are shown in the Fig 5.3-3.

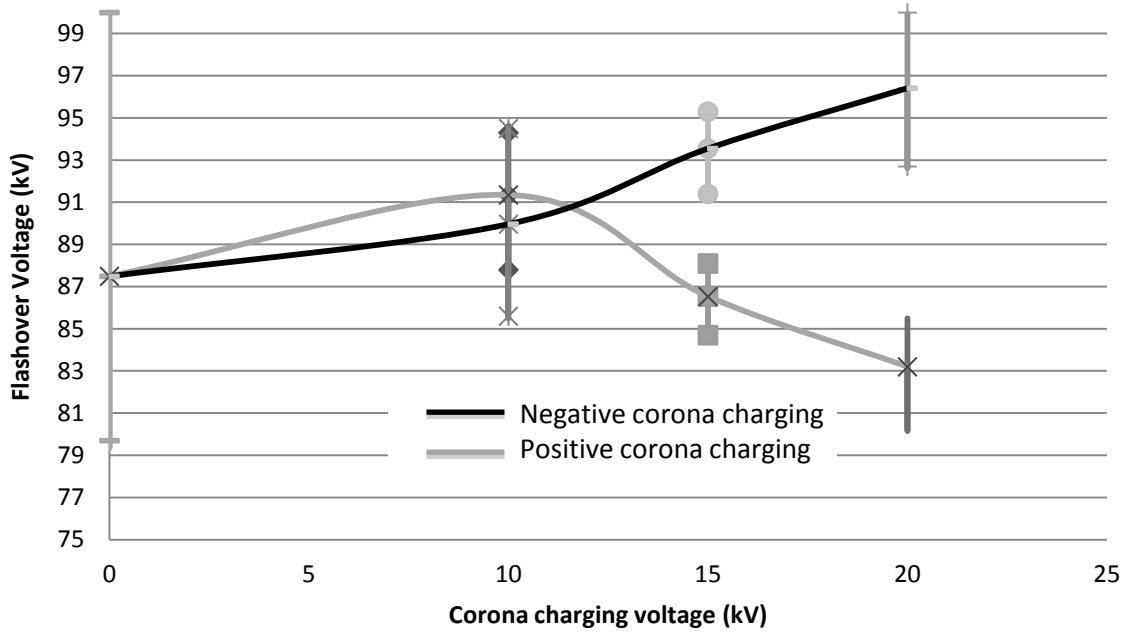


Figure 5.3-3: Flashover voltages with charges from corona only (note that the actual values of the flashover voltages are negative)

The reference at zero charging voltage represents the range of flashover voltages with clean surface. One can observe linear increase and decrease (for positive and negative charging, respectively) in the average flashover voltages with increasing charging voltages. A similar V-shaped characteristic for flashover voltages vs. deposited surface charge density were obtained as a result of simulations in [19]. According to discussion in [19], negative surface charges in combination with negative applied voltages cause a reduction of electric fields in the high field region (close to live electrode) that leads to higher flashover voltages. In case of positive charges, an increase in the magnitude of the electric field near the high field region can be found which causes a decrease in the flashover voltages as can be seen in fig 5.3-3. Increasing corona charging voltage for both the negative and positive polarity can deposit higher amount of surface charges, as discussed in detail in section 3.6, that may enhance the observed effect.

CHAPTER 6: CONCLUSIONS AND FUTURE WORK

6.1. Conclusions

Surface charge accumulation and its effect on the dc flashover performance of cylindrical polymeric insulators were investigated. The model insulator consisted of a glass fiber reinforced epoxy core (108 mm length, 30 mm diameter) covered with 4 mm thick layer of silicone rubber.

Surface potential distribution due to corona charging by the needle belt located at the center of the insulator was found to have a bell or saddle shape. The latter appeared when charging voltage exceed a certain threshold value. Time duration of the corona charging in the short run had no significant effect on the resulting surface potential distributions. When the insulator was pre-stressed by applying a high voltage (below flashover level), charges of the same polarity as the applied stress voltage had a dominant character near the live electrode and changed into opposite polarity mid-way along the insulator. Different flashover events deposit own charges and the resulting distributions didn't depend on the initial conditions on the insulator surface. Potential distributions due to combined effect of corona and pre-stressing or corona and flashover were not a simple addition of the individual potential distributions, but resulted in a totally different picture.

The surface potential decay measurement curves have been presented in different formats such as potential vs. time and log potential vs. log time to suggest a qualitative interpretation of the initial stage of the decay and also to discuss the cross-over phenomena.

The flashover voltages were measured for different conditions of charging of the insulator. The flashover voltages were found to be affected by the presence of surface charges despite of its origin and polarity. The dc flashover voltages with corona charges were investigated for three different scenarios: clean sample, charged by preceding flashover and pre-stressed sample. The three cases were investigated at both polarities and for different magnitudes of the corona charging voltage. Statistical variations for breakdown voltage were found to be in a limited range for the charged sample while they were in a comparatively wide range for clean sample.

It was found that combined charging produces practically no effect on the averaged dc flashover voltages while the influence was clearly seen when a clean sample was directly charged with external corona. In this case, dc flashover voltages (negative) increased with increasing negative charging voltages whereas reduced at positive charging.

6.2. Future work

Even though surface potential measurements are easy and fast to perform using electrostatic voltmeters, the quantification of surface charge magnitudes is not always simple. Analytical and numerical relations should be carefully considered in order to obtain meaningful values. Surface potential to surface charge conversion for flat samples requires simple analytical relations, but cylindrical and other geometries involve complex numerical calculations. This project opens a new window to select a suitable method for potential to charge conversion. Once it is achieved, the simulation studies can be further performed to investigate the effect of charges on the flashover performance and the results can be compared with the experimental observations.

The projected work related to surface charges and its effect on the flashover voltage was performed on a single type of model insulator. Similar studies can be performed on real insulators or on material samples having different properties.

References

1. F. Wang, Q. Zhang, Y. Qiu, E. Kuffel, "Insulator surface charge accumulation under DC voltage", IEEE International Symposium on Electrical Insulation, 2002, pp. 426 – 429, 7-10 Apr 2002.
2. F. Messerer, M. Finkel, W. Boeck, "Surface charge accumulation on HVDC – GIS - Spacer", IEEE International Symposium on electrical insulation, Boston, MA USA, April 7-10, 2002.
3. T. Nitta, K. Nakanishi, "Charge accumulation on Insulating Spacers for HVDC GIS", IEEE Transaction on Electrical Insulation, Vol. 26, No. 3, pp. 418-427, 2002.
4. Toomer R., Lewis T.J., "Charge Trapping in corona-charged Polyethylene films", Journal of physics D: Applied physics, Vol. 13, No. 7, pp. 1343-1355, 1980.
5. Baum E.A., Lewis T.J., Toomer R., "Decay of electrical charge on polyethylene films", Journal of Physics D: Applied Physics, Vol. 10, No. 4, pp. 487-497, 1977.
6. Mebrathu, Meleke Semere, "Charges on Polymeric Insulators and their effect on flashover characteristics", Master thesis, 2011.
7. E. Kuffel, W.S. Zaengl, J. Kuffel, "High Voltage Engineering Fundamentals", Pergamon Press, 1984.
8. Giacometti J.A., Oliveira O.N. Jr., "Corona charging of polymers", IEEE Trans. On Electrical Insulation, Vol. 27, No. 5, pp. 924-943, 1992.
9. Kumara S., Serdyuk Y.V., Gubanski S.M., "Charging of polymeric surfaces by positive impulse corona", IEEE Trans. On Die. And Elec. Insu., Vol. 16, No. 3, pp. 726-733, June 2009.
10. M. M. Shahin, "Nature of Charge Carriers in negative Coronas", Appl. Opt. Suppl. Electr. Photogr., Vol. 82, pp. 106-110, 1969.
11. M. M. Shahin, "Mass – Spectrometric Studies of Corona Discharges in air of Atmospheric Pressures", J. Chem. Phys., Vol. 43, pp. 2600-2605, 1966.
12. Kumara S., Serdyuk Y., Gubanski S., "Surface Charge Decay on Polymeric Materials under Different Neutralization Modes in Air", IEEE Trans. On Die. And Elec. Insu., 2011(in press)
13. Chinoglia D.L., Leal Ferreria G.F., Giacometti J.A., Oliveria O.N. Jr., "Corona-triode characteristics: on effects possibly caused by the electronic component", 7th International Symposium on Electrets, pp. 255-260, 1991.
14. Chen G., "Anomalous phenomena in solid dielectrics under high electric fields", IEEE 9th International Conference on the properties and Applications of Dielectric Materials, pp. 954-960, 2009.
15. Molinie P., Llovera P., "Surface potential measurement: Implementation and interpretation", IEEE Conf. Publ. No. 473, Eighth International Conference on Dielectric Materials, Measurements and Applications, pp. 253-258, 2000.
16. Sjöstedt H., "Electric Charges on Insulator Surfaces and their Influence on Insulator Performance", Licentiate Thesis, Chalmers University of Technology, Göteborg, Sweden, ISSN 1652-8891, No. 34/2008, 2008.
17. Maciej Dr., Noras A., "Non-Contact Surface charge/voltage measurements fieldmeter and voltmeter methods", Trek Application Note, 2002.
18. Ootera H., Nakanishi K., "Analytical method for evaluating surface charge distribution on a dielectric from capacitive probe measurement-application to a

- cone-type spacer in ± 500 kV DC-GIS”, IEEE Trans. On Power Delivery, Vol. 3, No. 1, pp. 165-172, 1988.
19. Kumara S., “Electrical charges on polymeric insulator surfaces and their impact on withstand performance”, Licentiate Thesis, Chalmers University of Technology, Göteborg Sweden, ISSN 1652-8891, Technical report no 55/2009, 2009.
 20. Blennow J., Sörqvist T., “Effect of Surface charge on the flashover voltage of polymeric material”.
 21. Montano R., Sjostedt H., Serdyuk Y., Gubanski S., “Effect of surface charges on the flashover voltage characteristics of polymeric materials: comparison between theory and practice”, Annual Report Conference on Electrical Insulation and Dielectric Phenomena, pp. 368-371, 2007.
 22. M.A. Abdul-Hussain, K.J. Cormick, “Charge storage on Insulation Surfaces in air under unidirectional Inpulse conditions”, IEE Proceedings on Physical Science, Measurement and Instrumentation, Management and Education, Vol. 134, No. 9, pp. 731-740, 1987.
 23. S. Haridoss, M.M. Perlman, C. Carlone, “Vibrationally excited diatomic molecules as charge injectors during corona charging of polymer films”, Journal of Applied Physics, Vol. 53, No. 9, pp. 6106-6114, 1982.
 24. Llovera P., Molinie P., “New methodology for surface potential decay measurements: application to study charge injection dynamics on polypropylene films”, IEEE Trans. Dielectrics and Electrical Insulation, Vol. 11, No. 6, pp. 1049-1056, Dec. 2004.
 25. Chen G., Zhao J., Zhuang Y., “Numerical modeling of surface potential decay of corona charged polymeric material”, IEEE International Conference on Solid Dielectrics (ICSD), pp. 1-4, 2010.
 26. Gustavsson, T. G., “Silicone Rubber Insulators - Impacts of Material Formulation in Coastal Environment”, Doctor of Philosophy Thesis, Chalmers University of Technology, Göteborg, Sweden, ISBN 91-7291-128-X, 2002.
 27. Skuckenholz C., Lequitte P., Gamlin M, Connell R., “Overview of Test requirements on HVDC apparatus and resulting impacts on UHVDC Testing systems”.
 28. P. Llovera, P. Molinic, A. Soria, A. Quijano, “Measurement of electrostatic potentials and electric fields in some industrial applications”, Journals of electrostatics, pp. 457-461, 2009.

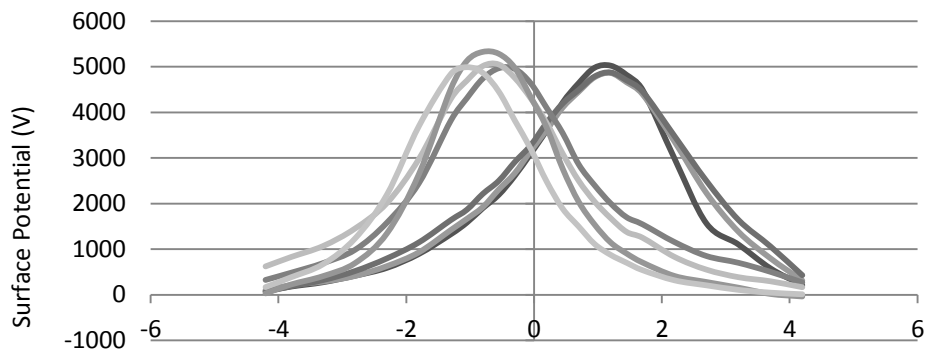
Appendixes

Appendix: A

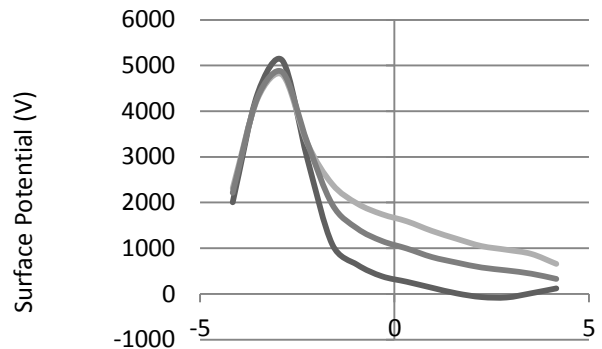
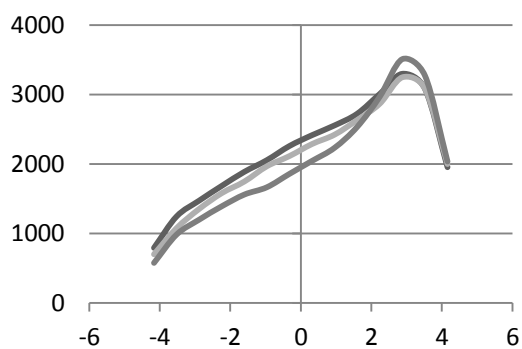
A1: Position study

The following figures show the surface potential distribution for grounded insulator sample with only charging from the corona belt at different polarity and magnitudes.

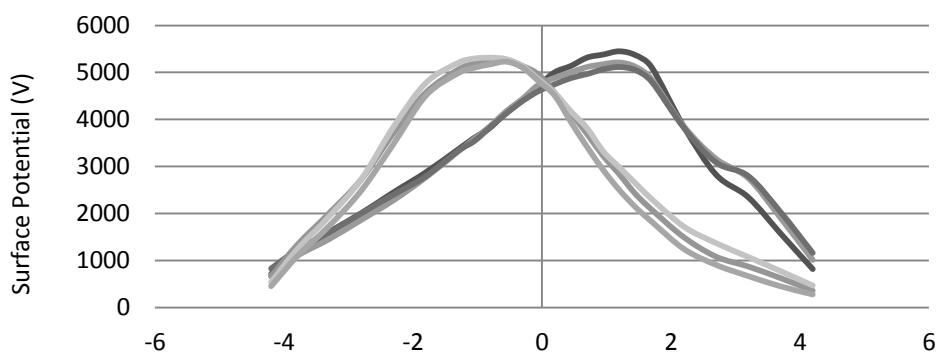
10 kV at ± 1 cm from the middle



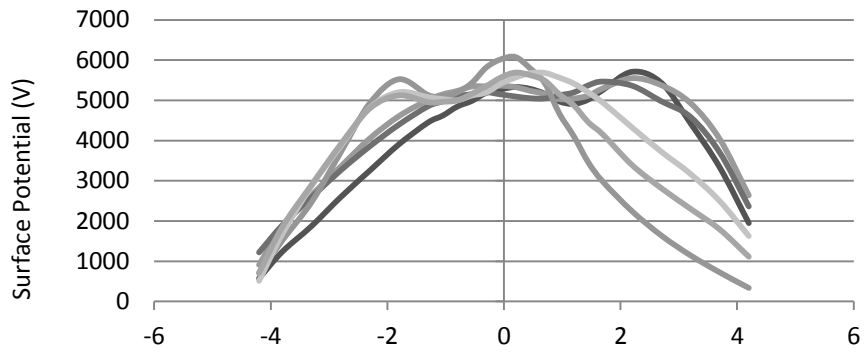
10 kV at ± 3 cm from the middle



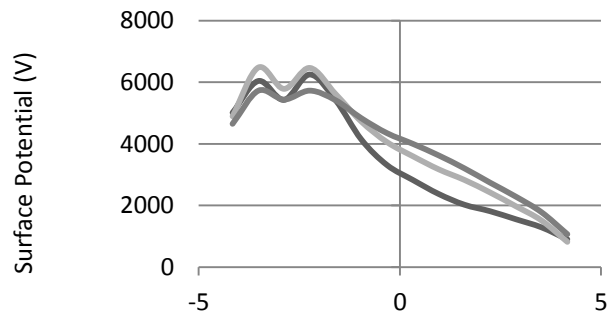
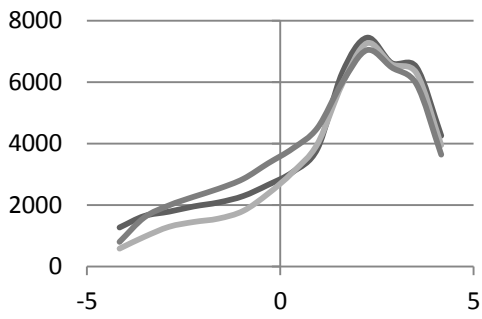
12 kV at ± 1 cm from the middle



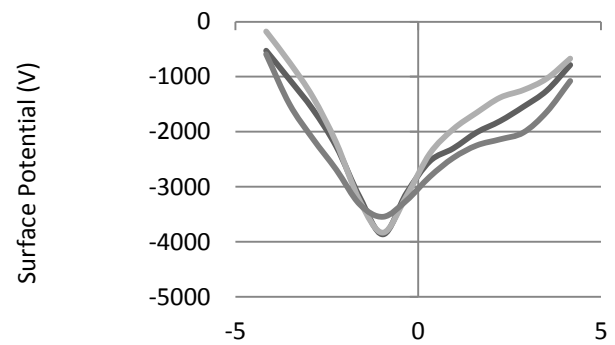
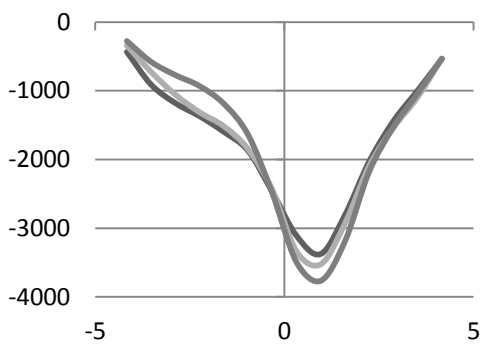
15 kV at ± 1 cm from the middle



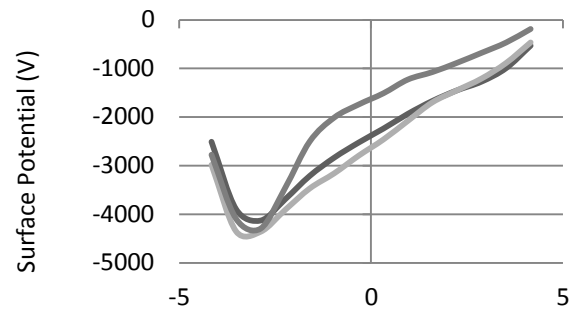
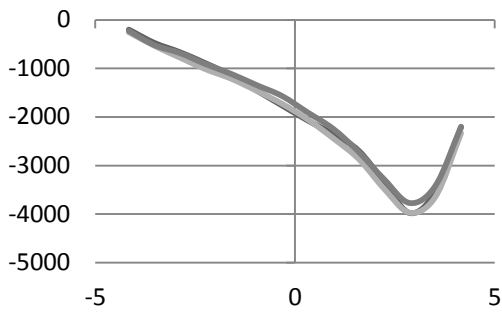
15 kV at ± 3 cm from the middle



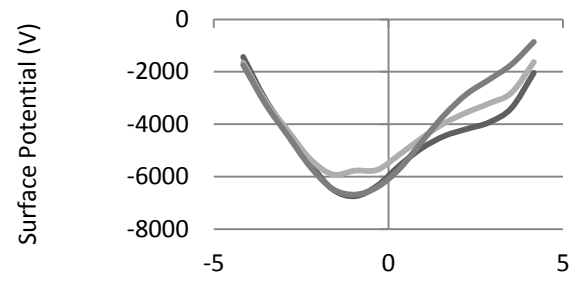
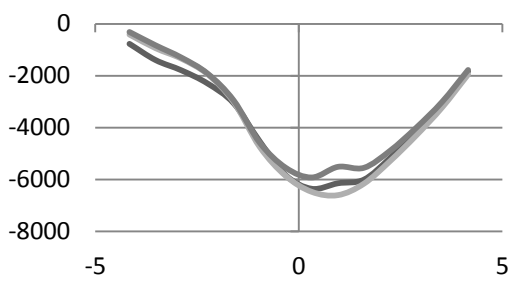
-10 kV at ± 1 cm from the middle



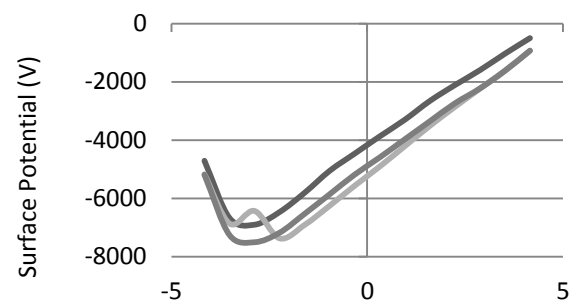
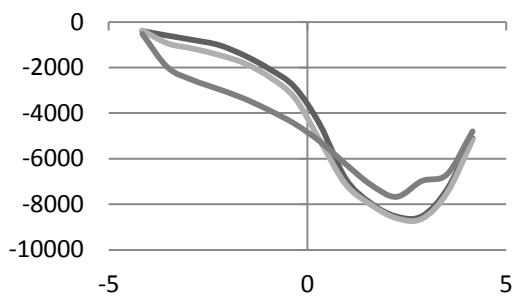
-10 kV at ± 3 cm from the middle



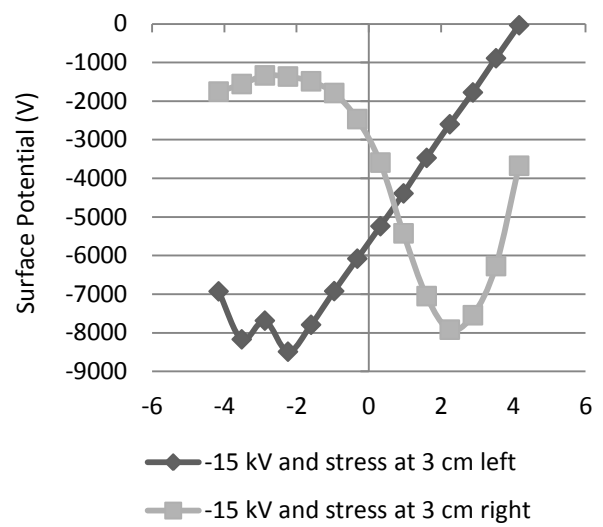
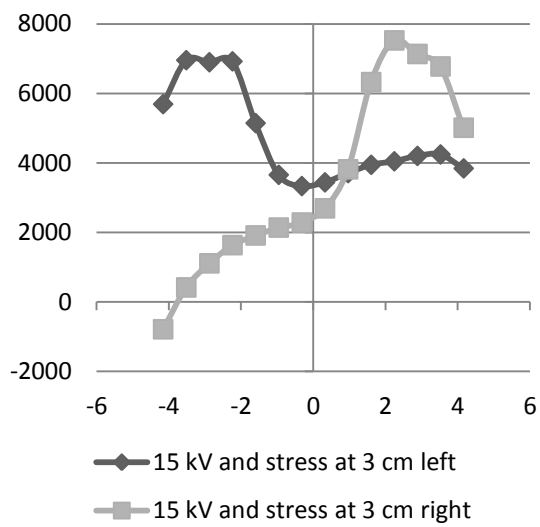
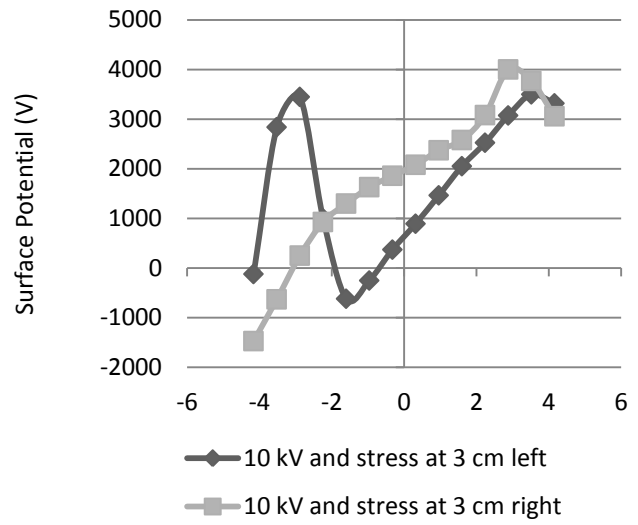
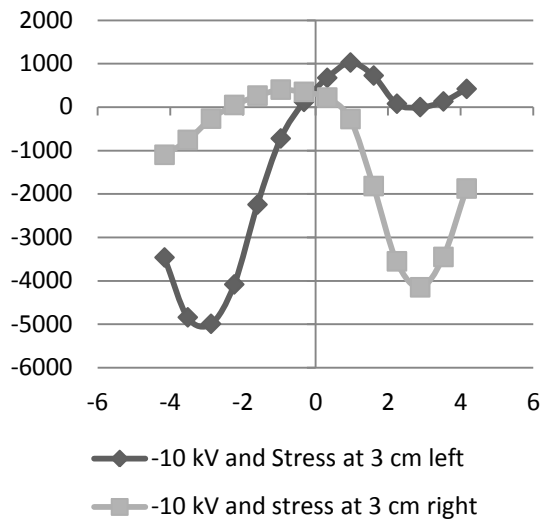
-15 kV at ± 1 cm from the middle



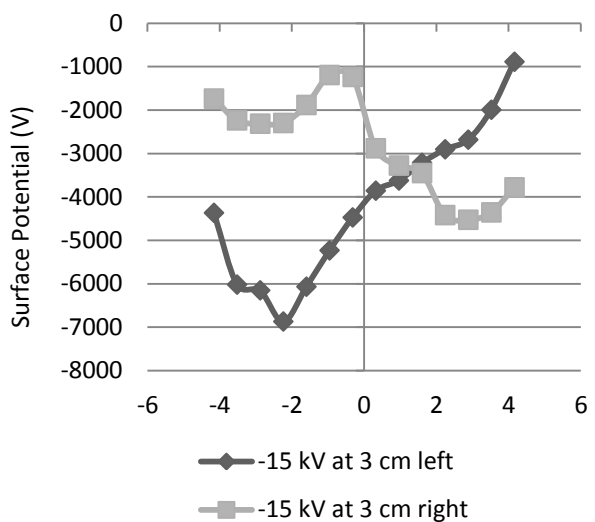
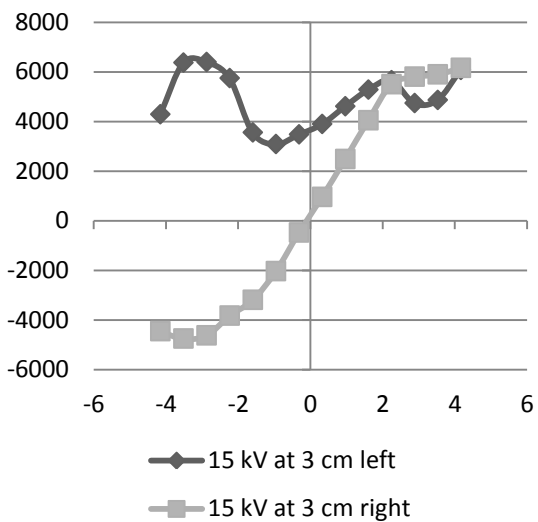
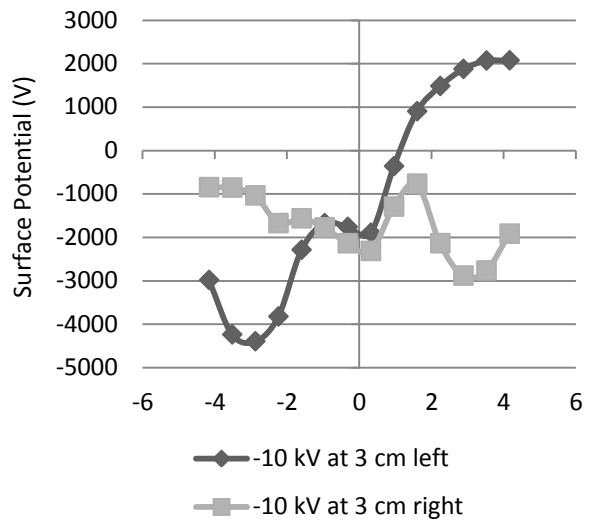
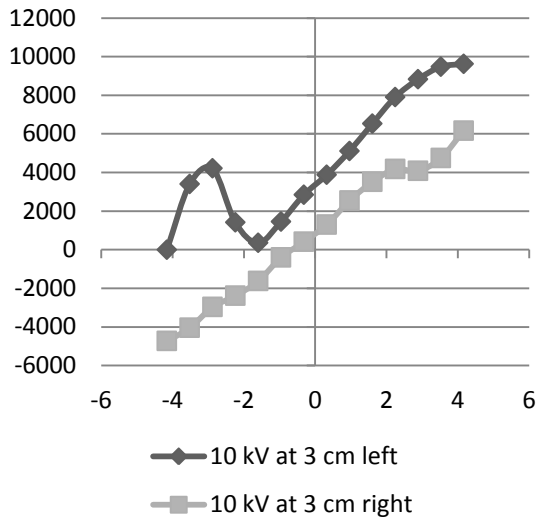
-15 kV at ± 3 cm from the middle



A2: Charges from pre-stressing and corona



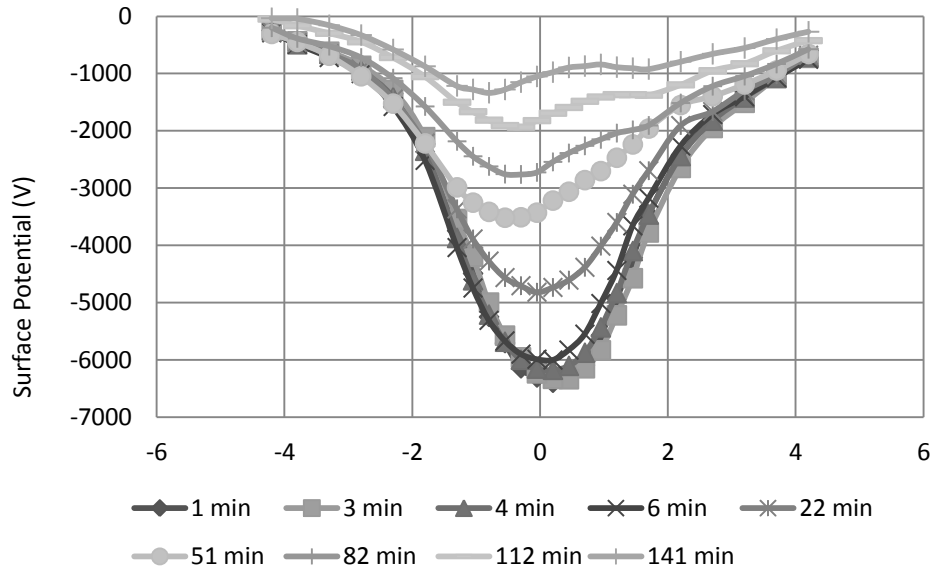
A3: Charges from previous flashover and corona



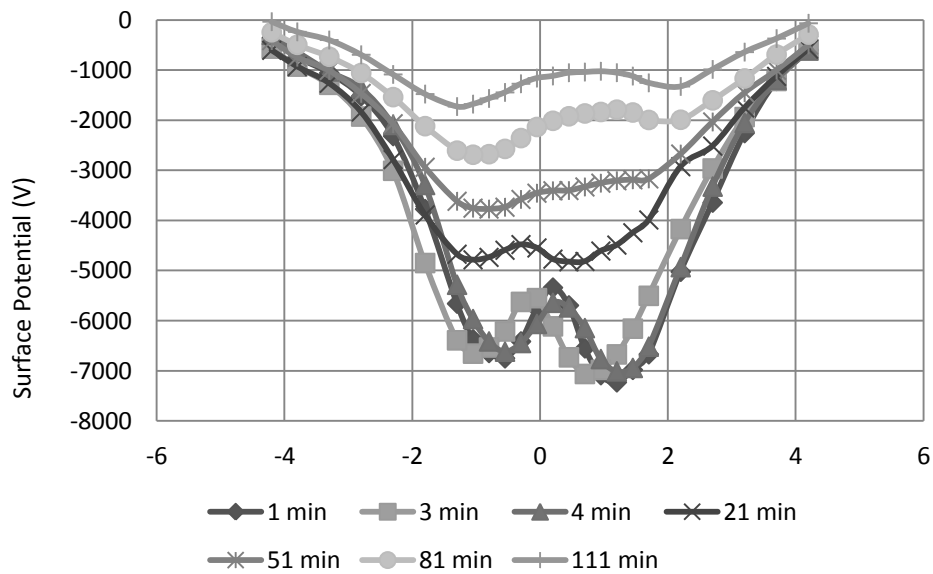
A4: Neutralization study

The following figures show the result of charge neutralization over time. Figures are for corona charging with -12 kV and -15 kV respectively.

-12 kV corona belt



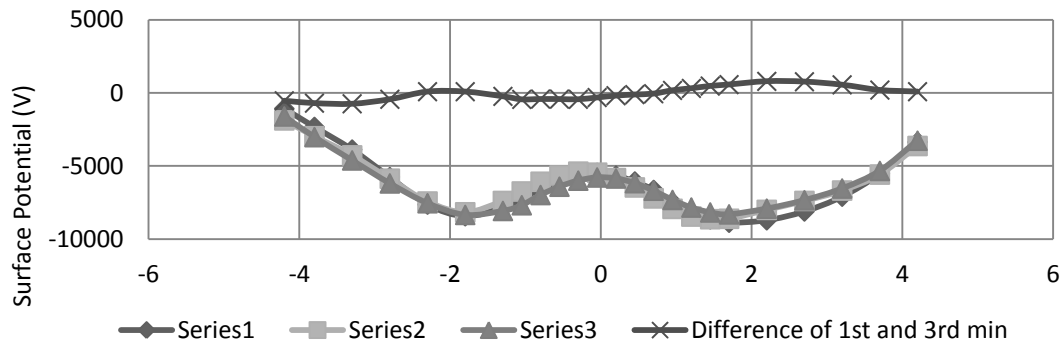
-15 kV corona belt



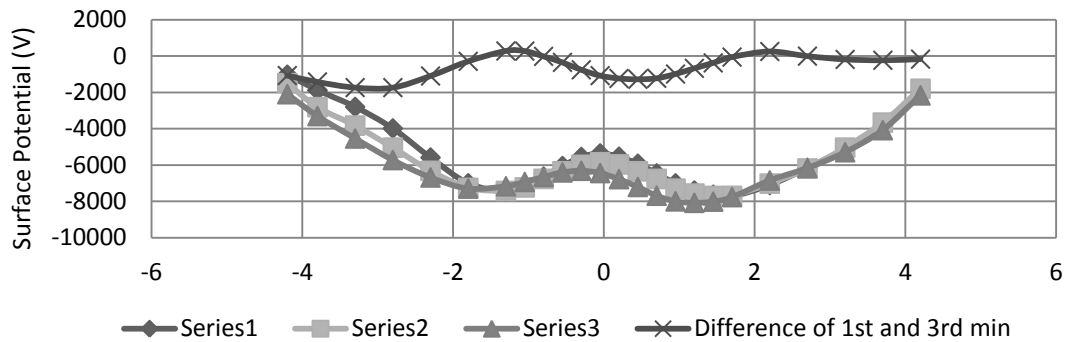
A5: Decay in first 3 minutes

The following figures show the potential distribution during 3 minutes after the charging was completed. These sets of studies were conducted to establish an experimental time range and to keep uniform experimental guidelines. Charging was done on a grounded insulator sample. Charging time was 2 minutes for each case.

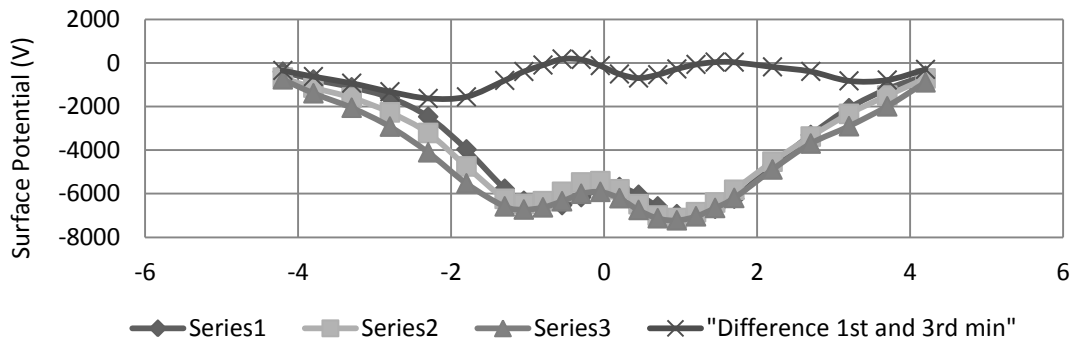
-20 kV charging



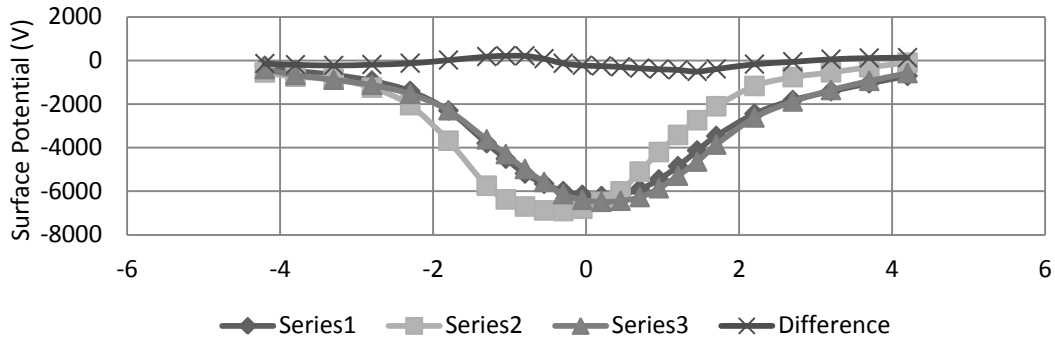
-18 kV charging



-15 kV charging



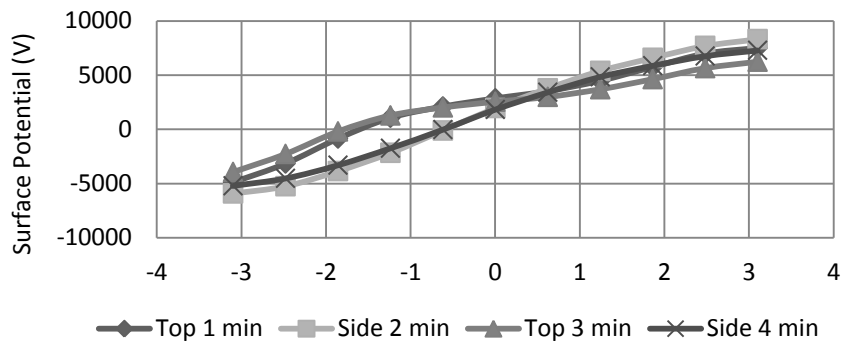
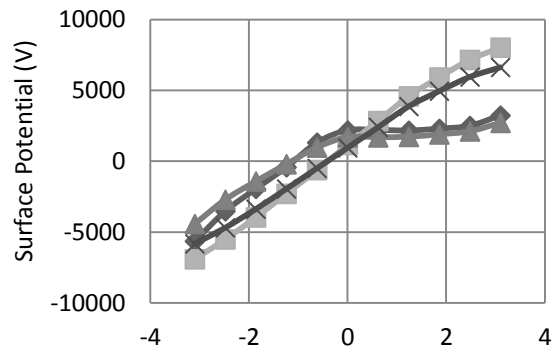
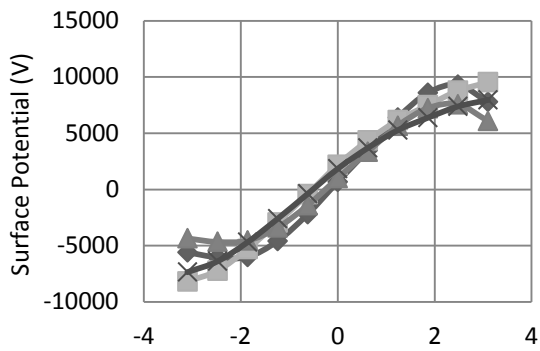
-12 kV charging



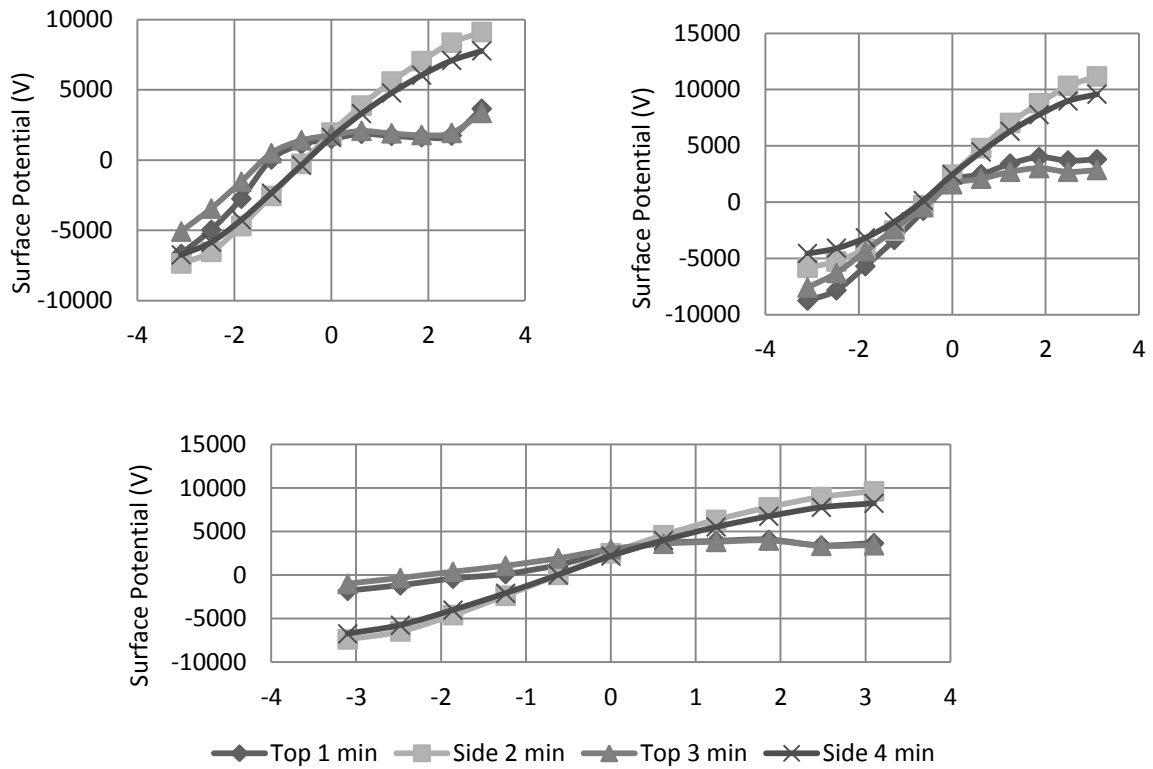
A6: Surface potential at different sides of the insulator sample

The following figures show the results of scanning the insulator surface at different sides, after it was subjected to charging with corona belt for 2 minutes.

Clean case

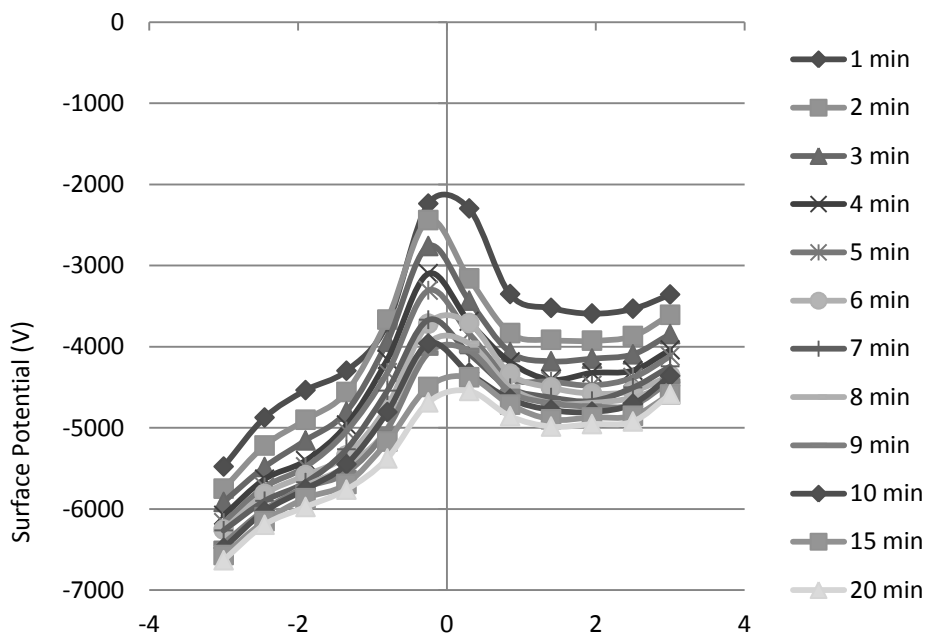


Stressed case



A7: Live scanning at -10 KV

This study shows the result of charge decay in the first 15 minutes while the electrodes at the both ends of the insulator sample were at -10 kV potential. Initially the insulator sample was charged with corona belt at -10 kV for 2 minutes.



Appendix B

FOV Values

Following tables show the FOV values (in kV) for 3 sets of tests conducted (Unclean, Clean, Stress), which are discussed in chapter 5.

Unclean Test		
Negative 10 KV	Negative 15 KV	Negative 20 KV
78.1	83	85.6
81.8	77.8	81.5
81.7	83.9	78.7
79.6	80.7	79.4
80.1	82.5	80.6
85.7	79.8	85.3
Clean Test		
Positive 10 KV	Positive 15 KV	Positive 20 KV
89.2	87.2	85.2
94.3	87.5	85.3
87.8	84.7	81.7
91.1	88.1	81.3
93	85.5	80.2
92.7	86.2	85.5
Stress Test		
Positive 10 KV	Positive 15 KV	Positive 20 KV
92.5	88.7	86.3
91.5	87.9	84
91.7	88.3	83.2
93.2	88.2	84.7
90.8	86.9	88.9
93	86.2	87.1

Unclean Test		
Positive 10 KV	Positive 15 KV	Positive 20 KV
82.5	79	77.1
80.4	79.7	81.2
79	76.6	76
78	81.5	75.5
78.1	76.5	76.1
78.6	77.7	78.8
Clean Test		
Negative 10 KV	Negative 15 KV	Negative 20 KV
88.7	95.3	95.3
94	93.2	100
85.6	94.5	100
94.5	91.4	97.1
88.4	94.3	93.4
88.6	92.6	92.7
Stress Test		
Negative 10 KV	Negative 15 KV	Negative 20 KV
97	98.6	96.2
100	94.1	93
90.2	95.7	92.9
99.2	95.2	87.1
88.2	95.1	100
90.6	89.2	98.8

Reference FOV Values

Clean Reference (kV)	Unclean Reference (kV)
80	81.3
80.9	88.7
80.5	84.2
89.4	79.8
92	81.3
81.9	83.8
79.7	82.1
93.9	84.6
96.6	80.6
100	83.3

Appendix C

Matlab Codes

This code was used for formatting data acquisition card values into useable values which can be imported into excel or any other plotting software for easy manipulation.

```
clear all
close all
clc
load 'test_2.txt'
tst(:,1)=test_2(:,2);
tst(:,2)=test_2(:,4);
temp=1;
flag=0;
flag2=0;
for t=1:1:length(tst(:,1))
    if(tst(t,2) < 1 )
        if (flag == 0)
            if (flag2==0)
                check(temp,1)= tst((t-3),1);
                temp=temp+1;
                flag2=1;
            end
            check(temp,1)=tst((t+4),1);
            temp=temp+1;
            flag=1;
        end
    end
    if(tst(t,2)>=1)
        flag=0;
    end
end
array=check*4000;
success=xlswrite('/Users/refath/Documents/check.xls',array)
%xlswrite('CHECK.xls',check);
```